environmental microbiology

Environmental Microbiology (2014) **16**(7), 1982–2003 doi:10.1111/1462-2920.12331

EBR1 genomic expansion and its role in virulence of *Fusarium* species

Wilfried Jonkers,[1†] Henry Xayamongkhon,[1] Matthew Haas,[1] Chantal Olivain,[2] H. Charlotte van der Does,[3] Karen Broz,[4] Martijn Rep,[3] Claude Alabouvette,[2] Christian Steinberg and H. Corby Kistler[1,4*]

[1]*Department of Plant Pathology, University of Minnesota, 1991 Upper Buford Circle St. Paul, MN 55108, USA.*

[2]*UMR 1347 Agroécologie, INRA, BP 86510, F-21065 Dijon cedex, France.*

[3]*Plant Pathology, Swammerdam Institute for Life Sciences, University of Amsterdam, Science Park 904, 1098 XH, Amsterdam, The Netherlands.*

[4]*USDA-ARS, Cereal Disease Laboratory, 1551 Lindig Street, St. Paul, MN 55108, USA.*

Summary

Genome sequencing of *Fusarium oxysporum* revealed that pathogenic forms of this fungus harbour supernumerary chromosomes with a wide variety of genes, many of which likely encode traits required for pathogenicity or niche specialization. Specific transcription factor gene families are expanded on these chromosomes including the *EBR1* family (Enhanced Branching). The significance of the *EBR1* family expansion on supernumerary chromosomes and whether *EBR1* paralogues are functional is currently unknown. *EBR1* is found as a single copy in *F. graminearum* and other fungi but as multiple paralogues in pathogenic *F. oxysporum* strains. These paralogues exhibit sequence and copy number variation among different host-specific strains and even between more closely related strains. Relative expression of the *EBR1* paralogues depends on growth conditions and on the presence of the single *EBR1* gene in the core genome. Deletion of *EBR1* in the core genome in different *F. oxysporum* strains resulted in impaired growth, reduced pathogenicity and slightly reduced biocontrol capacities. To identify genes regulated by *EBR1*, the transcriptomes of wild-type and Δ*ebr1* strains were compared for both *F. oxysporum* and *F. graminearum*. These studies showed that in both species, *EBR1* regulates genes involved in general metabolism as well as virulence.

Received 8 August, 2013; accepted 6 November, 2013. *For correspondence. E-mail hckist@umn.edu; Tel. (+1) 6126259774; Fax (+1) 6516495054. †Present address: Department of Plant and Microbial Biology, University of California, Berkeley, 341A Koshland Hall, Berkeley, CA 94720-3102 USA.

Introduction

In recent years, whole genome sequencing has been applied to pathogenic fungi to gain insight into their genetic potential. Together with different forward and reverse genetics methods, this has led to identification of many pathogenicity genes and mechanisms by which fungi infect their hosts. *Fusarium* is a fungal genus comprised of many pathogens of economically important crops (Cuomo *et al*., 2007; Coleman *et al*., 2009; Ma *et al*., 2010). High-quality draft genome sequence assemblies have been obtained for several species including the cereal pathogen *F. graminearum* (*Fg*), mostly known for causing head blight in wheat and barley (Goswami and Kistler, 2004), and *F. oxysporum forma specialis* (f. sp.) *lycopersici* (*Fol*), which causes tomato wilt disease (Di Pietro *et al*., 2003; Michielse and Rep, 2009).

Interestingly, when the genomes of multiple *Fusarium* species were compared with each other, it became clear that the genome of sequenced strain *Fol* 4287 is considerably larger than those of *Fg* or other species. This expansion was attributed predominantly to the presence of supernumerary chromosomes (Ma *et al*., 2010). These chromosomes are not required for normal cellular processes nor present in sister species and probably were initially obtained via horizontal transmission. Chromosomes laterally transferred from a pathogenic strain to a non-pathogenic strain can convert the non-pathogen into a pathogen (Ma *et al*., 2010). Presence of many effectors or *SIX* (secreted in xylem) genes (Rep *et al*., 2004; Houterman *et al*., 2007; 2009) on these chromosomes explains their importance for habitat specialization by *Fol*. The gene content of supernumerary chromosomes consists further of transposons, predicted secreted proteins, carbohydrate-active enzymes and other genes specifically expressed during plant infection (Ma *et al*., 2010). The sequenced *Fol* strain 4287 contains four extra lineage-specific (LS) chromosomes: two small ones, including chromosome 14 that contains multiple *SIX* genes, and two larger ones that contain long segmental duplications (chromosomes 3 and 6). Besides these four,

large subtelomeric regions of chromosomes 1 and 2 also have coding regions not present in sister species.

EBR1 is a putative transcription factor (TF) gene that is present in multiple copies on supernumerary chromosomes of *Fol*. The *EBR1* gene was first identified by insertional mutagenesis in *Fg* and initially characterized in both *Fg* and *Fol* (Dufresne *et al*., 2008; Zhao *et al*., 2011). In *Fg*, *EBR1* proved to be required for normal radial growth and for spread through the wheat head (Zhao *et al*., 2011). In *Fol*, this gene is also required for normal radial growth (Zhao *et al*., 2011), but whether it plays a role in pathogenicity was not reported.

Until now, *EBR1* has been found to be present as a multicopy family only in *Fol* and another *Fo* strain pathogenic to *Arabidopsis thaliana* (*F05176*), (Ma *et al*., 2010; Thatcher *et al*., 2012). Presence of *EBR1* is restricted to the *Pezizomycotina* as a single copy in most species. In the rice blast pathogen, *Magnaporthe oryzae*, a tagged mutant (MGG_09263) of the gene exhibits reduced virulence and is impaired in normal appressorium and conidia formation (Jeon *et al*., 2007), suggesting *EBR1* functions in pathogenicity in multiple plant pathogens. *EBR1* contains a Zn_2Cys_6-domain, a fungal-specific TF domain first described in the Gal4 protein in *Saccharomyces cerevisiae* (Kraulis *et al*., 1992), and localizes to the nucleus in both *Fg* and *Fol* (Zhao *et al*., 2011).

Here, we show that *EBR1* has undergone genomic expansion in several *F. oxysporum* lineages and analyse expression of the paralogous copies during vegetative growth and plant infection. Further, deletion mutants of *EBR1* were used to identify their possible targets in *Fol* as well as in *Fg* by transcriptome analysis.

Results

EBR1 is present in multiple copies in Fol

As noted earlier, at least seven potential *EBR1*-like paralogues may be present in *Fol* 4287 (Zhao *et al*., 2011). To locate all copies of the *EBR* gene family in *Fol* 4287, a Basic Local Alignment Search Toll (BLAST) (Altschul *et al*., 1997) search with *FgEBR1* was performed using the Broad Institute webserver (http://www.broadinstitute.org/annotation/genome/fusarium_group/MultiHome.html). Initially nine paralogues of *EBR1* in *Fol* were retrieved. The nine genes fall into four groups based on sequence similarity (Tables 1 and 2). The gene present as one copy with locus ID FOXG_05408 is designated *FoEBR1*. This gene was deleted in the previous study and is present on chromosome 7. This chromosome shows extensive synteny to chromosome 5 of the sister species *F. verticillioides* (Ma *et al*., 2010) and is therefore considered part of the core genome. FOXG_14277, present as a single copy as well, resides on chromosome 14, the small supernumerary chromosome. FOXG_14277 is designated *FoEBR2.* The three completely identical copies from the third group have locus ID numbers FOXG_06927, FOXG_16083 and FOXG_16925, and are designated as *FoEBR3*. FOXG_06927 and FOXG_16083 are each located on a repeated segment on chromosome 3, one of the two large supernumerary chromosomes. FOXG_16925 is located on chromosome 6, the other large supernumerary chromosome, on a genomic region that is a duplicated segment of chromosome 3. The four identical copies from the last group have locus ID numbers FOXG_12612, FOXG_12561, FOXG_13979 and FOXG_17064, and are designated as *FoEBR4*. FOXG_12612 and FOXG_12561 are located on chromosome 3, and FOXG_13979 and FOXG_17064 on chromosome 6. The latter two are located on the same duplicated segment as described for *EBR3* FOXG_16925. In the previous study, FOXG_12561 and FOXG_13979 were not reported probably due to a sequence gap of 352 base pairs (bp) in the middle of the genes. The chromosomal locations of the nine *EBR* genes are depicted in Fig. 1A.

We sequenced complementary DNA (cDNA) amplicons of each *EBR* gene in order to verify the presence of the two introns around the Zn_2Cys_6-domain and, where possible, the start of the open reading frame (ORF). Doing so, an extra intron of 83 bp in *EBR4* was found 33 bp after the putative ATG start codon. We inspected the sequences of the other three paralogues, and similar introns were found. Both *EBR2* and *EBR3* have an 82 bp long intron 26 bp after the putative ATG start codon. This intron was

Table 1. Nine *EBR* genes from *F. oxysporum* f. sp. *lycopersici* (*Fol*) strain 4287 with designated group and chromosomal location.

Gene locus ID	*EBR* group	Chromosome
FOXG_05408	*FoEBR1*	7
FOXG_14277	*FoEBR2*	14
FOXG_06927	*FoEBR3*	3
FOXG_16083	*FoEBR3*	3
FOXG_16925	*FoEBR3*	6
FOXG_12612	*FoEBR4*	3
FOXG_12561	*FoEBR4*	3
FOXG_13797	*FoEBR4*	6
FOXG_17064	*FoEBR4*	6

Table 2. Nucleotide similarities scores for each *EBR* paralogue.

Similarity at nucleotide level (%)	*EBR1*	*EBR2*	*EBR3*	*EBR4*
EBR1	100.00			
EBR2	78.60	100.00		
EBR3	77.86	91.91	100.00	
EBR4	76.86	70.83	70.98	100.00

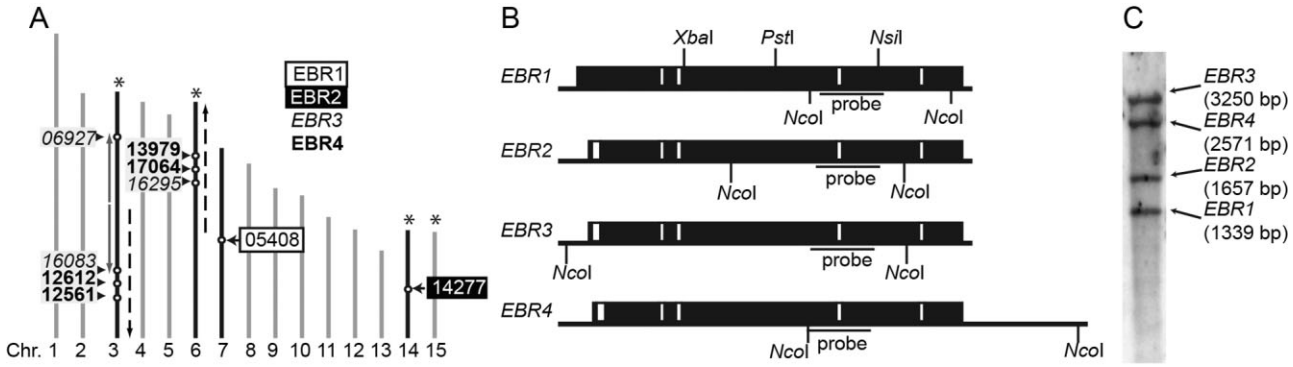

Fig. 1. Chromosomal distribution and gene models of the *EBR* gene family in *Fol* 4287.
A. Predicted chromosomal locations of the different *EBR* gene copies are displayed as a white dot on the chromosome. Each dot is indicated by the locus ID name (arrow). *EBR1* = white box, *EBR2* = black box, *EBR3* = *italic* and *EBR4* = **bold**. The chromosomes (Chr.) that contain *EBR* genes (#3, 6, 7 and 14) are black, the other ones grey. Dispensable chromosomes (#3, 6, 14 and 15) are marked with an asterisk (*). Grey arrows illustrate the chromosomal segmental duplication in chromosome 3, and dashed black arrows illustrate chromosomal segmental duplications of chromosomes 3 and 6. The directions of the arrows mark the sequence orientation.
B. Schematic gene models of *EBR1*, *2*, *3* and *4*. Black parts represent exons, white parts introns. The position of the probe and the *Nco*I recognition sites are depicted. For *EBR1*, the recognition sites of the enzymes used for the construction of truncated versions are given as well.
C. Southern blot of *Nco*I digested genomic DNA of *Fol* 4287 hybridised with the *EBR* probe showing four distinct bands, each representing one of the *EBR* paralogue groups.

not found in *EBR1*. In Fig. 1B, the gene models are given for the four *EBR* genes.

Unlike the overall coding sequence similarities (76–78%, Table 2), sequences upstream of the ATG differ greatly between *EBR1* and its paralogues. When the 1000 bp upstream of the predicted ATG from *EBR1* were aligned to the 1000 bp upstream of the predicted ATG from any of the other *EBR* genes, no alignment was found, and sequence similarity was at a maximum of only 23% (grey bar, Fig. S1A). This is in strong contrast with the alignment among the 5′ regions of the three *EBR* paralogues on LS regions. The sequence of about 650 bp upstream of the ATG of *EBR4* aligns strongly to both *EBR2* and *EBR3* 5′ regions (sequence similarity of 81%, Fig. S1A, black bars). No such strong sequence alignment was found further upstream between *EBR4*, and *EBR2* or *EBR3* (sequence similarity of 28%, Fig. S1A, diagonal striped bar). Interestingly, *EBR2* and *EBR3* share longer segments of their upstream region. Almost the entire region of 1000 bp 5′ of *EBR2* is found perfectly duplicated 5′ of *EBR3* (sequence similarity of 95%). The total alignment runs further up to approximately 4000 bp upstream. Differences between the two sequences lie in a stretch that is inserted in the upstream region of *EBR2* or lost in *EBR3* (Fig. S1A, white portions in the black bars).

Alignment of the predicted proteins from the four manually annotated *EBR* copies with *Fg*Ebr1, revealed highly similar protein sequences. Merely the ORF start sites and the N-terminal regions differ somewhat between the copies (Fig. S1B).

Of the four different *Fol* Ebr versions, Ebr1 (FOXG_05408) shows the highest similarity to *Fg*Ebr1 (89%). The other versions show similarity to a lesser extent; 74%, 76% and 70% for Ebr2, Ebr3 and Ebr4 respectively. *Fo*Ebr1 also shows the highest similarity (95%) to the single Ebr of *F. verticillioides*, encoded by FVEG_02723 (because of the incomplete sequence at the C-terminus of this gene, only the protein sequence encoded by the first 2999 bp could be aligned). Among the *Fo* paralogues, Ebr2 and Ebr3 show the highest degree of amino acid similarity to *Fo*Ebr1, 80% and 81%, with Ebr4, at 74%, showing a somewhat lower similarity. These data are in agreement with *FoEBR1* being the orthologue of the single *EBR1* in *Fg* and *Fv*. *EBR2*, *EBR3* and *EBR4*, located in LS regions, may have originated either through gene duplication before divergence of *Fo*, *Fg* and *Fv* (followed by loss in *Fg* and *Fv* clades) or through acquisition by *Fo* via horizontal transfer (Ma *et al*., 2010).

To confirm the presence of the four *EBR* genes in *Fol* 4287, a Southern blot experiment was performed. The C-terminal parts of the genes contain a highly conserved region where primers could be designed that align completely to each of the four different *EBR* genes and amplify a product of similar length from each of the four genes (Fig. 1B). We digested the DNA of *Fol* 4287 with restriction enzyme *Nco*I that cuts in each gene at a different position (Fig. 1B), causing the probe to hybridize to fragments of different sizes corresponding to the different *EBR* paralogues in *Fol* 4287. This verified the presence of each paralogue in the *Fol* 4287 genome (Fig. 1C).

Table 3. *F. oxysporum* f. sp. *lycopersici* (*Fol*) strains used in this study.

Name	Origin	Race	VCG	Reference
4287	Spain	2	0030	Ma *et al*., 2010
MN-25	Florida, USA	3	0033	Gale *et al*., 2003
MM10	Arkansas, USA	3	0033	Marlatt *et al*., 1996
007	France	2	0030	Mes *et al*., 1999
DF038	California, USA	2	0031	Cai *et al*., 2003
DF023	California, USA	2	0035	Cai *et al*., 2003

Paralogues of EBR1 in pathogenic forms of F. oxysporum *associate with small LS chromosomes*

The sequenced *Fol* strain 4287 belongs to vegetative compatibility group (VCG) 0030 and is verified to be to a race 2 isolate. Race is determined by the presence and/or absence of avirulence genes, which by way of their protein product, cause recognition conferred by a corresponding resistance gene present in the tomato host (Lievens *et al*., 2009). Vegetative compatibility between strains is determined by allelic identity at several unlinked genetic loci; only strains that are identical at all loci can form heterokaryotic mycelium and thus belong to the same VCG (Kistler *et al*., 1998). To determine whether the copy number and distribution of paralogous *EBR* genes is similar among different races and VCGs of *Fol*, we tested for the presence of paralogues in different strains by Southern blotting as in Fig. 1C. Strains tested were *Fol* 007 (Race 2, VCG0030), MN-25 (Race 3, VCG0033), MM10 (Race 3, VCG0033), DF023 (Race 2, VCG0035) and DF038 (Race 2 VCG0031), and non-pathogenic strain Fo47 (Table 3).

Figure 2A shows that strain 007 contains four different genes and has the same *Nco*I restriction pattern as strain 4287. Fo47, the non-pathogenic strain, contains only an *Nco*I band identical in size to *EBR1*, the copy on the core genomes. DNA from MM10 contains *Nco*I bands corresponding in size to *EBR1* and *EBR2*, and lacks the upper bands corresponding to *EBR3* and *EBR4*. MN-25 also contains *Nco*I bands corresponding in size to *EBR1* and *EBR2*, and lacks the two upper bands but contains a third, novel-sized band absent in other strains. This implies that this paralogue has a different sequence than the four *EBR* genes described from strain 4287. This copy is presumed to be different from *EBR1–4* and is called *EBR5*. Strains DF023 and DF038 show three *Nco*I bands corresponding in size to *EBR1*, *EBR2* and *EBR4*, and both lack the upper band corresponding to *EBR3*. This shows that all pathogenic *Fol* strains tested have at least one extra *EBR* gene, which in this case is *EBR2*. Presence of the different *EBR* paralogues does not seem to correlate with race nor VCG. MN-25 and MM10, for example, are in the same VCG, and 007 and DF0–38 are of similar race, but each has different *EBR* paralogues.

To determine whether *EBR1* paralogues are also present in strains of *F. oxysporum* with different host specificities, a similar Southern hybridization experiment was conducted. These strains included pathogens of cotton (*Fov*), melon (*Fom*), pea (*Fop*) and banana (*Foc*), a crown rot pathogen of tomato (*Forl*) and a strain isolated from human blood (*Foh*) (Table 4). The Southern hybridization pattern was found to be different for each strain (Fig. 2A). A band corresponding in size to *EBR1* was present in all strains. A band corresponding in size to *EBR2* was only present in *Fom*, *Forl*, *Foh* and *Fop.* Bands similar in size to *EBR3* and *EBR5* were noted only in *Forl*, and *EBR4* was not conserved among any of the other tested *F. oxysporum* strains. Several bands corresponding to sizes different than the ones found for *Fol* were present in all other tested *F. oxysporum* strains. The total number of distinct *EBR* paralogues among these strains varies between two and five (Fig. 2A).

In order to correlate the presence of these unique *EBR* bands in many of these strains to chromosomal loci, we separated chromosomes by contour-clamped homogeneous electric field (CHEF) electrophoresis. The same probe used for paralogue identification in genomic Southerns was used to hybridize to blots of CHEF gels. The strains previously examined and another strain pathogenic to cabbage and Arabidopsis (*Foca*) were included (Table 4). CHEF gels (Fig. 2B upper panel) show that almost each strain contains a unique electrophoretic karyotype with small, unique chromosomes. As previously noted (Ma *et al*., 2010), *Fol* 4287 contains two unique small

Table 4. Other *F. oxysporum* strains used in this study.

NRRL #	Strain name	Abbreviation	Forma speciales	Host	Reference
54002	Fo47	–		Non-pathogenic	Fravel *et al*., 2003
25433	–	*Fov*	Vasinfectum	Cotton	–
26406	–	*Fom*	Melonis	Melon	–
54006	II5 (tropical race 4)	*Foc*	Cubense	Banana	Fourie *et al*., 2009
26381	CL57	*Forl*	Radicis-lycopersici	Tomato	Rosewich *et al*., 1999
32931	FOSC 3-a	*Foh*	– (human)	Human	O'Donnell *et al*., 2004
37622	HDV247	*Fop*	Pisi	Garden pea	–
54008	PHW808	*Foca*	Conglutinans	Cabbage	–

NRRL, Northern Regional Research Laboratory.

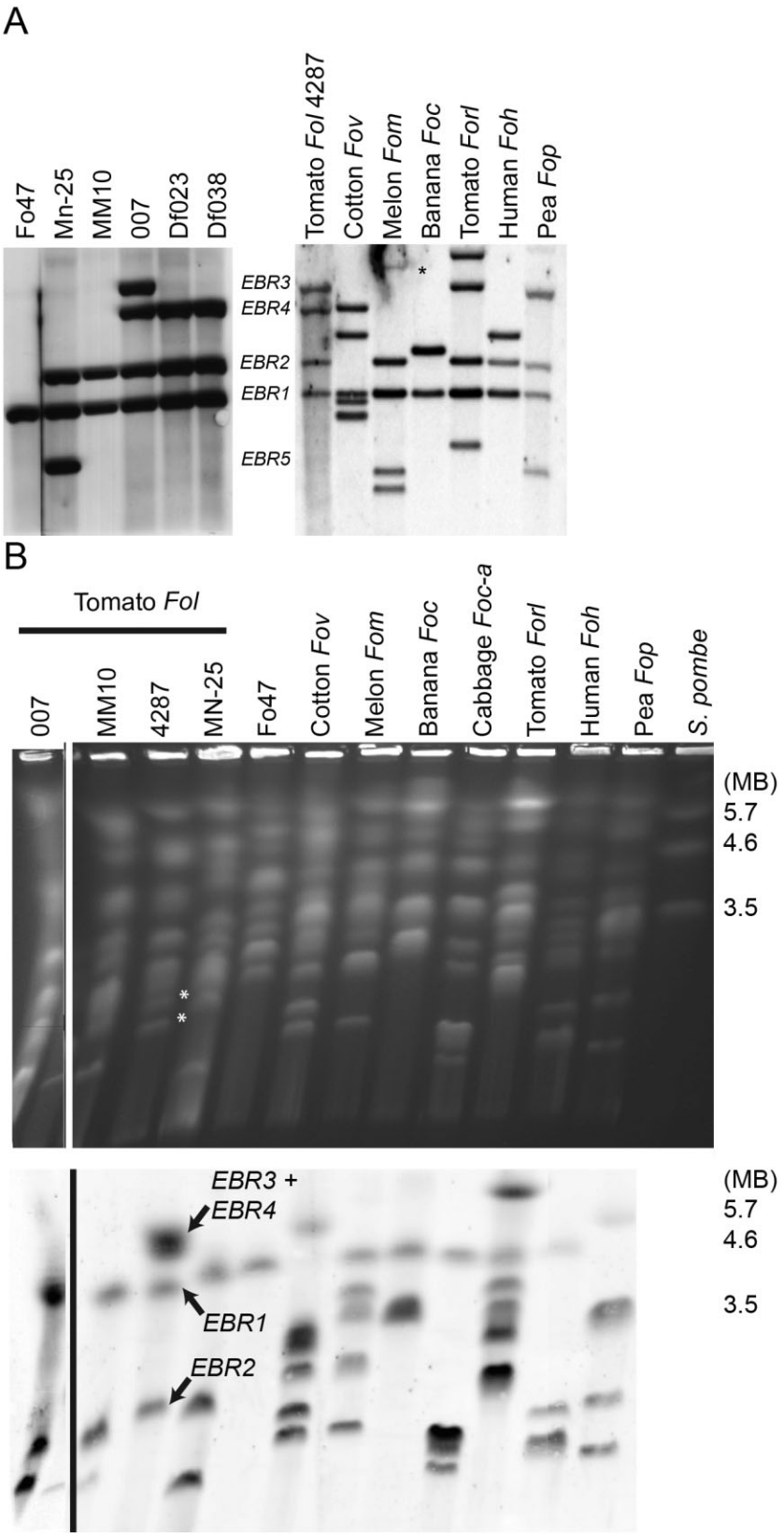

Fig. 2. The *EBR* diversity and chromosomal location in *Fo* strains.
A. Southern blot of *Nco*I digested genomic DNA of Fo47 and five *Fol* strains (left panel) and six *Fo* strains of different host specificities (Table 3) and *Fol* 4287 (right panel) hybridized with the *EBR* probe. *Fol* 4287 is included to show the hybridization pattern of the four *EBR* genes. For each *EBR* paralogue in *Fol*, the name is given at the right side of the blot.
B. CHEF gel (upper panel) showing the chromosomal distribution and corresponding Southern blot (lower panel) with 12 *Fo* strains (Tables 2 and 3) hybridised with the *EBR* probe. On the right, chromosomes of *S. pombe* are run as chromosomal size standards (MB = megabases), and the same size markers are also given on the right side of the blot. The chromosomes of *Fol* 4287 that contain *EBR* genes are marked with an arrow and respective *EBR* gene is indicated.

chromosomes, numbered 14 and 15, which are present as the two bands indicated with an asterisk. As expected, the *EBR* probe hybridized in this lane to one of the size of chromosome 14 (*EBR2*, see arrow), to one of chromosome 7 (*EBR1*, see arrow) and to the two larger chromosomes, chromosomes 6 and 3 that are poorly separated in CHEF electrophoresis because of their large and similar size (*EBR3 + 4*, see arrow, Fig. 2B lower panel). For most other strains (Fig. 2B lower panel), the *EBR* probe hybridized to a chromosome the same size as chromosome 7 in *Fol* 4287 – containing the conserved *EBR* homologue in the core genome. However, for *Fov* and *Fop*, a chromosome larger than chromosome 7 is observed. It is possible that these larger chromosomes also correspond to *Fol* 4287 chromosome 7 but with additional DNA segments or that *EBR1* in these strains resides on a different chromosome.

In other tomato pathogenic strains, the *EBR* probe hybridizes to a chromosome similar in size to chromosome 14 in *Fol* 4287, and hybridization to other small chromosomes was observed. MM10 and MN-25 contain two small chromosomes hybridizing with the probe, presumably containing *EBR2*. In MN-25, *EBR5* also may be present on one of the small chromosomes. Interestingly, for strain 007, which contains all four copies, hybridization is observed only to two small chromosomes and to chromosome 7 but not to larger ones similar in size to chromosomes 3 and 6 in *Fol* 4287. This is in line with the smallest chromosome in *Fol* 007, which can be horizontally transferred, containing sequences corresponding to *Fol* 4287 chromosomes 3 and 6 (Ma *et al*., 2010).

For the non-pathogenic strain Fo47, hybridization occurred only to chromosome 7 corresponding to the location of *EBR1*. Most other pathogenic strains contain extra copies of *EBR* genes on small chromosomes (e.g. ones that are as small or smaller than chromosome 14 of *Fol* 4287). *Foh* and *Foca* have these extra genes exclusively on the small chromosomes. Only for *Foc* II5 are small chromosomes not visible; instead the extra *EBR* copies probably are present as multiple paralogues on one or more chromosomes of ~3.5 Mb in size. For *Fov*, *Fom* and *Fop*, the *EBR* probe hybridizes to both small and larger chromosomes and for *Forl*, hybridization to several larger chromosomes was seen. Altogether, extra copies of *EBR* are present in all pathogenic *F. oxysporum* strains (but not the non-pathogenic strain Fo47), and the sequence, copy number and chromosomal location of these extra genes are variable.

Deletion of EBR1 causes a growth phenotype in Fol *strains independent of EBR copy number*

As mentioned before, the deletion of *EBR1* in *Fg* results in reduced radial growth on complete rich medium (Zhao *et al*., 2011), and this phenotype was also observed, although to a lesser extent, in the *Fol* 4287 Δ*ebr1* strain. To investigate whether this phenotype is observed for other Δ*ebr1* mutants of tomato pathogenic strains, we deleted *EBR1* in *Fol* strains 4287, MM10, MN-25, 007, Df023 and Df038, and in non-pathogenic *Fo* strain Fo47 using *Agrobacterium tumefaciens* mediated transformation (ATMT – see Experimental procedures). We also attempted to delete *EBR2* in *Fol* 4287 because this was another paralogue presumably present as a single copy. However, after screening several hundred transformants for an *EBR2* deletion, we did not obtain any mutant strains.

We grew the wild-type strains, Δ*ebr1* mutants and ectopic transformants on nutrient poor medium, Czapex Dox agar (CDA) and on rich medium, potato dextrose agar (PDA). On CDA (Fig. 3A), Δ*ebr1* mutants have a distinct phenotype, with reduced radial growth and a macroscopic appearance whereby hyphae appear to adhere to each other and grow as strands rather than as individual hyphae as seen with wild-type and ectopic transformants. For most Δ*ebr1* mutants, the phenotypes are similar, except for the Fo47 mutants that show less severe symptoms even though, for this genotype, *EBR1* is the sole copy of this gene family. On PDA (Fig. 3B), the growth phenotypes of Δ*ebr1* mutants in 4287 and MM10 were not as pronounced as the phenotype of growth inhibition observed with Δ*ebr1* mutants in Df023, 007, MN-25 and Fo47. In addition to impaired growth, the Δ*ebr1* mutants of Df038 also displayed a macroscopic phenotype similar to the ones observed on CDA. This growth phenotype on agar plates for all strains might be due to the impaired hyphal apical dominance as suggested for Δ*ebr1* in *Fg* (Zhao *et al*., 2011). However, when tested in liquid complete medium (CM) for 48 h, no obvious growth defect in terms of biomass of *Fol* 4287 Δ*ebr1* was observed when compared with wild type (data not shown). When wild-type 4287 and two individual Δ*ebr1* mutants were further tested in a Biolog assay (Khalil and Alsanius, 2009) for growth on 95 different carbon sources, no obvious differences in overall growth in the 96 wells (total optical density value/plate) was observed for the first 3 days (Fig. S2). Slightly reduced growth of the two mutants was observed after 4 days when compared with wild type. When we then inspected single carbon sources that might contribute to this reduced growth after 4 days, the Δ*ebr1* mutants showed reduced growth (≥ twofold) compared with wild type on N-acetyl-D-glucosamine, m-Inositol, mannitol, β-methyl-D-glucoside, D-trehalose, turanose, L-glutamate and adenosine (Fig. S2 and Table S1). On the other hand, Δ*ebr1* mutants grew better (≥ twofold) compared with wild type on D-saccharic acid, succinate mono-methyl ester and L-alanyl-glycine (Fig. S2 and Table S1). These results suggest that Ebr1

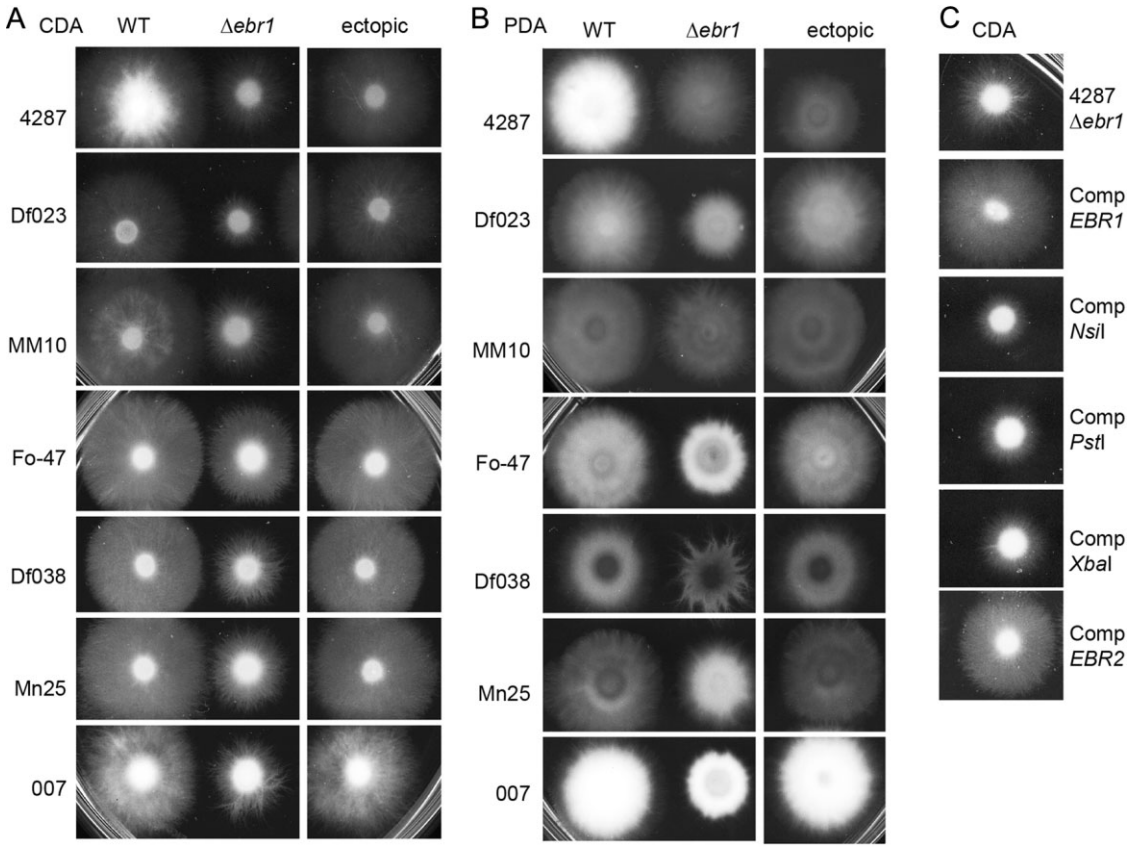

Fig. 3. Growth phenotypes of wild type, Δ*ebr1*, ectopic and complement mutant strains on poor and rich medium.
A. Wild type (WT), Δ*ebr1* and an ectopic mutant of seven different *F. oxysporum* strains are grown on poor medium (CDA).
B. Wild type (WT), Δ*ebr1* and an ectopic mutant of seven different *F. oxysporum* strains are grown on rich medium (PDA).
C. Δ*ebr1*, *EBR1* complementation mutant (Comp *EBR1*), three truncated complementation mutants (Comp *Nsi*I, *Pst*I and *Xba*I) and *EBR2* complementation mutant with *EBR2* placed behind the *EBR1* promoter (Comp *EBR2*) were grown on poor medium (CDA) to assess restoration of the Δ*ebr1* growth phenotype.

may regulate utilization of certain carbon sources required for full growth on agar plates.

EBR1 and EBR2 can complement EBR1 function when expressed from the EBR1 promoter but truncated versions of EBR1 cannot

Next, we determined whether we could complement the phenotype of *Fol* 4287 Δ*ebr1* on CDA with *EBR1* and with *EBR2* driven by the *EBR1* promoter as well as with three different truncated versions of *EBR1* (Fig. 3C). The truncated versions were made in order to ascertain the function of the different domains of the protein. The first truncation (Comp *Xba*I) deletes the entire C-terminal domain excluding the portion encoding the Zn_2Cys_6-domain (from an *Xba*I site on, Fig. S1B). The second truncated protein (Comp *Pst*I) extends about 900 bp past the first one and deletes only the second fungal specific TF domain (from a *Pst*I site on Fig. S1B). The function of this fungal specific TF domain found in many fungal TFs has been elusive to date. The third truncation (Comp *Nsi*I) deletes only the final ± 750 bp leaving both TF domains intact (from an *Nsi*I site on Fig. 1B and Fig. S1B).

The complete ORF of *EBR1* or the three different truncated ORF versions with ± 1000 bp upstream and downstream were cloned into plasmid pRW1p and used to transform a Δ*ebr1* strain. Multiple transformants were obtained and confirmed by polymerase chain reaction (PCR) (data not shown). Growth on CDA was restored with the full gene but not with any of the truncated versions (Fig. 3C). This suggests that at the minimum, the highly conserved C-terminal part (last 750 bp), while containing no obvious functional domain, is required for function.

We also transformed the Δ*ebr1* mutant with a wild-type copy of *EBR2*, but as expected, because *EBR2* was already present in this background, no restoration of normal growth was observed (data not shown). This suggests that native *EBR2* and apparently also *EBR3* and *EBR4* cannot compensate for loss of *EBR1* function during growth on CDA. We then transformed the Δ*ebr1* mutant with *EBR2* behind the *EBR1* promoter and found

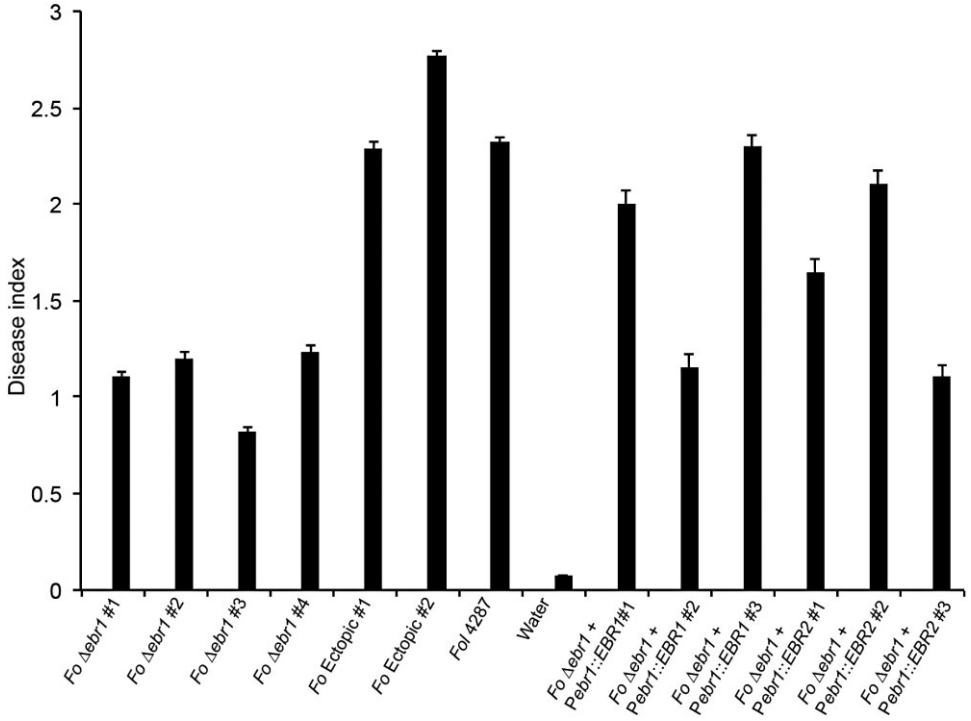

Fig. 4. The deletion of *EBR1* causes a minor decrease in pathogenicity towards tomato plants. Average disease index of each strain is shown in a histogram. (0 = healthy plant, 1 = plant showing thickening of hypocotyls but no vessel browning, 2 = plant showing one or two brown vessels and more than four true leaves, 3 = plant showing three or more brown vessels and more than four true leaves, 4 = plant showing four or less true leaves or severely diseased or dead plant). Disease indices of 20–40 plants were scored 3 weeks after inoculation. Error bars represent the standard error of the mean.

restoration of growth (Fig. 3C). This suggests that the protein encoded by *EBR2* can only functionally replace the protein encoded by *EBR1* when placed behind the *EBR1* promoter.

Loss of EBR1 causes impaired plant infection by Fol

In order to find out whether *EBR1* also may function in pathogenicity, a bioassay comparing mutants and complemented strains was conducted. We scored inoculated plants after 3 weeks for disease symptoms according to a disease index scale. Plants mock-inoculated with water showed no symptoms. The two ectopic strains were pathogenic to tomato to the same extent as wild type; plants showed browning of the xylem vessels and wilting symptoms. The four independent Δ*ebr1* strains proved to be moderately impaired in pathogenicity (Fig. 4), All four Δ*ebr1* mutants show significantly lower ($P \leq 0.01$, Student's *t*-test) average disease indices than the wild-type or ectopic transformants (data not shown). For three of the four Δ*ebr1* mutants, plant weight is significantly higher ($P \leq 0.05$, Student's *t*-test) than with the wild-type or ectopic transformants, also indicating less disease (data not shown).

Next, we tested whether this pathogenicity phenotype could be restored by *EBR1* or *EBR2* expressed from the *EBR1* promoter. Using three independent *EBR1* complemented strains, we found substantial restoration to wild-type disease-causing levels with two of the three ($P \leq 0.05$, Student's *t*-test) and partial restoration with the other when compared with the Δ*ebr1* mutants. Using three independent *EBR2* complements, we found substantial restoration to wild-type disease-causing levels with one of the three ($P \leq 0.05$, Student's *t*-test) and partial restoration with the other two when compared with the Δ*ebr1* mutants (Fig. 4).

EBR1 has a minor role in conferring biocontrol properties during root colonization

Because only one copy of *EBR1* is present in the biocontrol strain Fo47, deletion of *EBR1* created an *F. oxysporum* strain without any *EBR* gene. Full deletion of *EBR1* in Fo47 has an effect on growth similar to *EBR1* deletion in other stains, in line with the inability of additional *EBR* genes in pathogenic strains to compensate for loss of *EBR1*. With this strain, we could investigate a potential role of *EBR1* in biocontrol. Biocontrol activity of Fo47 has been reported to be dependent on colonization of superficial cell layers, a capacity shared between pathogenic and protective strains, and independent of competition for putative penetration sites (Alabouvette

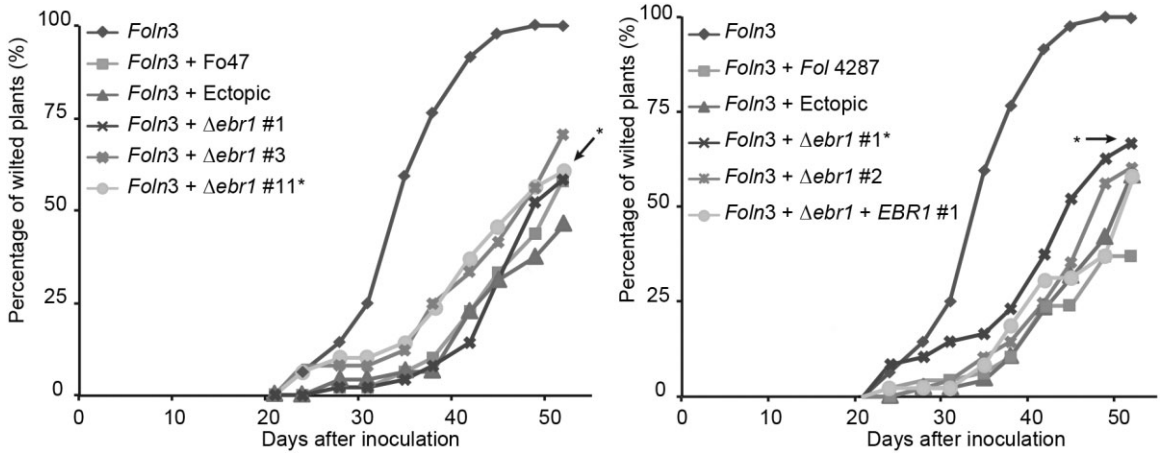

Fig. 5. The Δ*ebr1* mutants and their parental strains exhibit biocontrol activity on flax. The protective capacity of Δ*ebr1* and its parental strain were determined on flax. Flax cv. Opaline was inoculated with the pathogenic isolate *F. oxysporum* f. sp. *lini* 3 (*Foln*3) (1×10^3 conidia ml^{-1}) alone or in combination with the Fo47 [left graph (l)] or *Fol* 4287 [right graph (r)] wild-type strains or their respective *ebr1* mutants, ectopic or complement strain (1×10^5 conidia ml^{-1}). *Fusarium* wilt incidence is expressed as percentage of wilted plants. Black diamond = *Foln*3 alone, gray square = *Foln*3 and Fo47 (l) or *Fol* 4287 (r), black triangle = *Foln*3 and ectopic in Fo47 (l) or *Fol* 4287 (r), black cross = *Foln*3 and Δ*ebr1* #1 in Fo47 (l) or Δ*ebr1* #1 in *Fol* 4287 (r), grey cross = *Foln*3 and Δ*ebr1* #3 in Fo47 (l) or Δ*ebr1* #2 in *Fol* 4287 (r), gray circle = *Foln*3 and Δ*ebr1* #11 in Fo47 (l) or Δ*ebr1* #1 + *EBR1* #1 in *Fol* 4287 (r). The Δ*ebr1* strains that show significant differences in biocontrol abilities from their respective wild types are indicated with an asterisk (*) and arrow.

et al., 2009). Because a growth defect on agar plates was observed with the *EBR1* deletion mutants, root colonization might also be reduced, which in turn might impair the biocontrol properties. Both *Fol* and Fo47 exert biocontrol activity on flax when added in 100-fold excess relative to an *F. oxysporum* strain pathogenic towards flax, *F. oxysporum* f. sp. *lini* (Foln3). To determine whether the Δ*ebr1* mutants are able to protect flax against wilt disease like the wild-type strains, flax cultivar Opaline was treated with either a pathogenic isolate of Foln3 alone or in a 1:100 ratio with either the wild-type strain, an Δ*ebr1* mutant, an ectopic transformant or a complemented strain. The first wilt symptoms were observed 22 days after inoculation in the treatment with Foln3 and all the Foln3/mutant and Foln3/wild-type combination treatments. Disease incidence was reduced throughout the remaining portion of the experiment for Foln3/Δ*ebr1* mutants and Foln3/wild-type treatments compared with the Foln3 treatment alone: 52 days post-inoculation disease incidence was significantly reduced by the wild types Fo47 and *Fol*, and also by the ectopic and complemented transformants. For two Δ*ebr1* mutants in Fo47 and one in *Fol* 4287, similar reduced disease incidences compared with their respective wild types were determined. However, one Δ*ebr1* mutant strain in Fo47 and one in *Fol* 4287 showed significantly reduced biocontrol capacity (Fig. 5). The analysis of variance (ANOVA) performed on area under the disease progress curve (AUDPC) indicated that for the latter two strains, this difference was significant with a probability of 95%. We conclude that Δ*ebr1* mutants in either Fo47 or *Fol* 4287 are still able to protect flax against *Fusarium* wilt to similar extent or a slightly reduced extent compared the wild-type strains. The Δ*ebr1* mutant strains that have a slightly reduced biocontrol capacity might have been affected in the speed or intensity of root colonization.

Expression profiles of EBR genes during vegetative and infectious growth

To determine whether the expression of the different *EBR* genes varies under different growth conditions, the contribution of each *EBR* transcript relative to the total of *EBR* transcripts was examined in *Fol* 4287. Because the sequences of the four *EBR* paralogues are very similar, measuring transcript levels from each gene by quantitative PCR (qPCR) is unreliable; specific probes would be difficult to design and could lead to false-positives. Instead, we compared paralogue transcript levels using a PCR and restriction enzyme analysis (see Experimental procedures). We first amplified *EBR* genes from genomic DNA and determined the relative abundance of the different paralogues, which, according to the genome sequence, should for *Fol* 4287 amount to *EBR1* : *EBR2* : *EBR3* : *EBR4* = 1:1:3:4. We also determined the genomic ratios in this way for *Fol* 007, MM10 and Fo47. The latter shows, as expected, only the *EBR1* copy. MM10, which only contains *EBR1* and *EBR2*, shows a ratio of *EBR1* : *EBR2* = 1:2. This suggests that in MM10, *EBR2* is duplicated, and this confirms the results obtained with the CHEF gel and associated Southern (see discussion earlier). The ratio for 4287 was not as expected, namely:

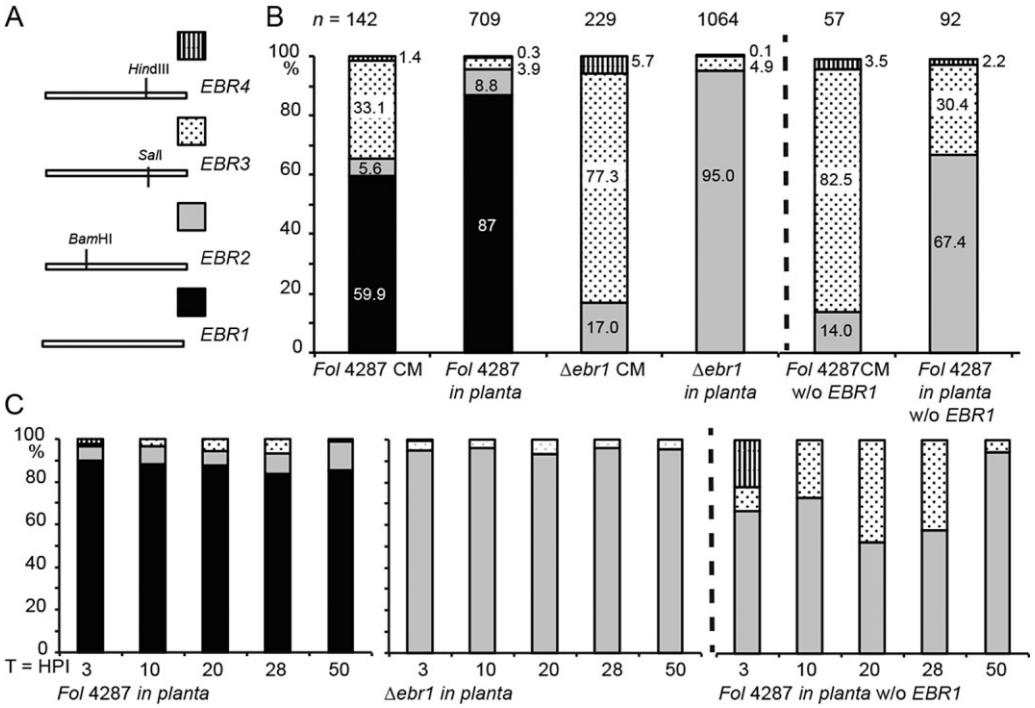

Fig. 6. *FoEBR* expression levels differ during growth in CM and *in planta* and between wild type and Δ*ebr1* mutant during growth *in planta*.
A. Schematic representation of the probe sequence of each *EBR1* paralogue containing either a *Bam*HI, *Sal*I or *Hin*dIII site in *EBR2*, *EBR3* and *EBR4* respectively.
B. Distribution of the *EBR* transcripts in percentages in wild-type *Fol* 4287 during growth in complete medium (CM) or *in planta* (left two columns), in Δ*ebr1* during growth in CM or *in planta* (middle two columns) and the distribution of *EBR2*, *EBR3* and *EBR4* in *Fol* 4287 during growth in CM or *in planta* when the percentages of *EBR1* are not taken into account (right two columns). The percentages for *EBR1* are given in black, *EBR2* in grey, *EBR3* in black dots and *EBR4* in black vertical stripes. The total number of transcripts analysed (n) is given above each column.
C. Distrubution of the *EBR* transcripts in percentages in wild type *Fol* 4287 during growth *in planta* at different hours post-inoculation (HPI) (left graph), in Δ*ebr1* (middle graph) and the distribution of *EBR2*, *EBR3* and *EBR4* in *Fol* 4287 during growth *in planta* when the percentages of *EBR1* are not taken into account (right graph). The percentages for *EBR1* are given in black, *EBR2* in grey, *EBR3* in black dots and *EBR4* in black vertical stripes.

EBR1 : *EBR2* : *EBR3* : *EBR4* = 1:1:3:2 (Chi-square test, $P < 0.01$). This suggests that *EBR4* may be present in two copies instead of four. It is possible that the two partial genes FOXG_12561 and FOXG_13979 results from an assembly error of the repeats that are located both on chromosomes 3 and 6, and are in fact not present in the genome. *Fol* 007 was previously determined to contain all four *EBR* genes, and the CHEF blot revealed that all extra copies are probably on small supernumerary chromosomes. In this strain, the ratio is *EBR1* : *EBR2* : *EBR3* : *EBR4* = 1:2:1:1 (Chi-square test, $P < 0.05$), indicating that *EBR2* is likely present in two copies and *EBR3* and *EBR4* as single ones.

Using cDNA clones derived from RNA, we similarly determined the ratio of transcripts for the *EBR* paralogues in *Fol* 4287 and the corresponding Δ*ebr1* mutant during growth in culture and after inoculation of tomato seedlings (see Experimental procedures). During growth of *Fol* 4287 in CM, we found that *EBR1* was the most abundant transcript captured as cDNA (± 60%), followed by *EBR3* (± 30%). Smaller proportions of *EBR2* (± 5%) and *EBR4* (± 1%) cDNAs were found (Fig. 6A). For the Δ*ebr1* mutant during growth in CM, we found the proportions of *EBR2*, *EBR3* and *EBR4* transcripts to be 17%, 77% and 6% respectively. This ratio is similar to the ratio of *EBR2*, *EBR3* and *EBR4* in wild type (Fig. 6A), suggesting that *EBR1* does not affect the expression ratios of the other three paralogues during growth in CM.

During root colonization and infection, however, different *EBR* transcript ratios were found. In the wild type, the majority of *EBR* transcripts inferred from cDNA abundance again was from *EBR1* but in higher percentages than in culture, between 83% and 91%. *EBR2* transcripts were between 6% and 14%, and *EBR3* between 0.5% and 7%. The *EBR4* transcript was not detected during growth on seedlings, with the exception of the first time point at 2% (Fig. 6A and B). In the Δ*ebr1* mutant during plant infection, the majority of the transcripts as measured by cDNA abundance correspond to *EBR2* and smaller numbers correspond to *EBR3*. No *EBR4* cDNAs were

detected. Clearly, in both wild type and Δ*ebr1* mutant, the contribution of *EBR2* and *EBR3* to the total *EBR* transcripts is reversed during plant colonization relative to *ex planta* growth, with *EBR2* becoming more dominant *in planta*. Still, in the wild-type *EBR1* remains the dominantly expressed *EBR* gene, even more so *in planta*.

FgEBR1 and FoEBR1 regulate predominantly different sets of targets

To gain more insight in the roles of *FgEBR1* and *FoEBR1* during growth in culture we conducted transcriptome (microarray) experiments with both wild types and Δ*ebr1* mutants of *Fg* and *Fo*. For this, we created *FgEBR1* deletion mutants via *Agrobacterium*-mediated transformation (see Experimental procedures). CM cultures were inoculated with conidia, and after 48 h, mycelium was collected and RNA was extracted and prepared for microarray analysis.

EBR1 seems to regulate genes positively as well as negatively. In *Fg*, 162 genes are expressed at more than fivefold lower levels in the Δ*ebr1* mutant compared with the wild type, whereas 68 are expressed at more than fivefold higher levels (Table S2). In *Fo*, 152 genes are expressed at more than fivefold lower levels in the Δ*ebr1* mutant compared with wild type, whereas 52 are expressed at more than fivefold higher levels (Table S3). Even though *Fg*Ebr1 and *Fo*Ebr1 regulate about the same number of genes directly or indirectly, the overlap of genes similarly regulated by both is rather small. Of the genes that are expressed ≥ fivefold higher in wild-type PH-1 compared with Δ*ebr1* in *Fg,* seven orthologues are also expressed ≥ fivefold higher in wild-type *Fol*4287 compared with Δ*ebr1* in *Fo* (Table S4). One of these seven genes encodes glucosamine-6-phosphate isomerase, an enzyme that catalyses the conversion of D-glucosamine 6-phosphate (GlcN6P) to D-fructose 6-phosphate and ammonia, the last step in the pathway for N-acetyl-glucosamine (GlcNAC) utilization. This may explain the impaired growth on N-acetyl-glucosamine of the Δ*ebr1* mutant in *F. oxysporum* observed in the Biolog assay. Another gene positively regulated by *EBR1* in both species encodes xylulose-5-phosphate phosphoketolase, a key enzyme of the pentose phosphate pathway. Three other positively *EBR1*-regulated genes in both *Fusarium* species encode a predicted MFS transporter, a methyltransferase and an oxygenase. The sixth gene encodes a protein similar to clock-controlled gene 9 from *Neurospora crassa*, which is a putative trehalose synthase (Shinohara *et al*., 2002). The seventh gene encodes a small (110 aa) secreted protein bearing 10 cysteine residues and found only in *Fusarium* species. The homology of this protein between *Fol* and *Fg* is mainly based on the conserved positions of the cysteines. *Fg* has two copies of this small cysteine-rich protein of which only one is expressed during growth in CM (Table S4). The only orthologue found to be up-regulated in both *Fo* Δ*ebr1* and *Fg* Δ*ebr1* encodes a trans-aconitate-2-methyltransferase (Table S4).

In addition to genes that are similarly regulated in *Fg* and *Fo*, seven genes are oppositely regulated at least fivefold by *EBR1* in *Fg* versus *Fo*. Five genes are expressed at higher levels in the Δ*ebr1* mutant of *Fg* but at lower levels in the mutant of *Fol*. One of these five encodes a protein similar to yeast Azf1, a TF that regulates genes involved in growth and metabolism (Slattery *et al*., 2006). Interestingly, in *Fol*, *EBR1* regulates the *AZF1* copy found on supernumerary chromosome 14. The other *AZF1* copy, FOXG_01564, is expressed to similar levels in the *Fol* wild type and Δ*ebr1* mutant. The other four encode for a nitrilase, an O-methyltransferase, an acyltransferase and a hypothetical protein. Two genes are expressed at higher levels in the *Fol* Δ*ebr1* mutant compared with wild type, but at lower levels than wild type in the *Fg* Δ*ebr1* mutant. Both genes encode putative oligopeptide transporters that share 34% total identity on the protein level (data not shown).

Genes differentially expressed between wild type and the Δ*ebr1* mutant were assigned to functional categories using the Functional Catalogue (FunCat) browser of the Munich Information Center for Protein Sequences (Ruepp *et al*., 2004). Genes with lower expression in the *Fg* Δ*ebr1* strain compared with *Fg* wild type were enriched in categories of metabolism and energy ($P \leq 0.01$) and over-represented were genes involved in glycolysis and gluconeogenesis (FunCat 02.01; $P = 6.28E-07$) and its regulation (FunCat 02.01.03; $P = 1.20E-05$) as well as C-compound and carbohydrate metabolism (FunCat 01.05; $P = 1.30E-06$) and subcategories (Table S5).

Genes that were expressed more highly in the *Fg* Δ*ebr1* strain compared with wild-type *Fg* were over-represented in functional categories of cell rescue, defence and virulence (FunCat 32; $P = 0.004$), heavy metal ion transport (Cu+, Fe3+, etc.) (FunCat 20.01.01.01.01; $P = 0.005$), and tryptophan metabolism (FunCat 01.01.09.06; $P = 0.008$) (Table S6). These data suggest that during growth in CM, *EBR1* in *Fg* positively regulates carbon metabolism and negatively regulates genes involved in defence.

To determine functional categories of genes regulated by *EBR1* in *Fol*, high identity homologues of genes found in *Fg*, if present, were determined and were used for analysis of FunCat enrichment. Of the 152 genes in the *Fol* Δ*ebr1* mutant that were expressed > fivefold lower than in the wild type, 119 had a close homologue in *Fg* and of the 52 expressed > fivefold higher than in the wild type, 48 had a homologue in *Fg*. In contrast with the categories identified in *Fg*, the 119 genes that were expressed at lower levels in the *Fol* Δ*ebr1* strain

compared with *FoI* wild type were enriched for functional categories of cell rescue, defence and virulence (FunCat 32; $P = 0.001$), virulence and disease factors (FunCat 32.05.05; $P = 8.57E-06$), toxins (FunCat 32.05.05.01; $P = 6.13E-05$), inorganic chemical agent resistance (e.g. heavy metals) (FunCat 32.01.03.03; $P = 0.002$), resistance proteins (FunCat 32.05.01; $P = 0.003$), detoxification (FunCat 32.07; $P = 0.003$)c and chemical agent resistance (FunCat 32.05.01.03; $P = 0.003$) (Table S7). Also, in contrast with the categories identified in *Fg*, the genes that are expressed at higher levels in the Δ*ebr1* strain compared with wild type were enriched for categories of metabolism (FunCat 01; $P = 1.57E-11$), cellular transport, transport facilities and transport routes (FunCat 20; $P = 3.94E-06$), energy (FunCat 2; $P = 1.10E-05$), and of protein with binding function or cofactor requirement (structural or catalytic) (FunCat 16; $P = 7.98E-04$) (Table S8).

In conclusion, *EBR1* in the two *Fusarium* species appears to regulate genes for metabolism and defense/virulence but in opposite ways. While a few genes are regulated similarly in both species, the gene sets regulated are largely non-overlapping.

Fg Δebr1 cannot spread through the rachis in spite of trichothecene toxin production

As shown previously, the *Fg* Δ*ebr1* mutant cannot spread from point inoculated spikelets to adjacent ones because it is halted at the rachis node (Zhao *et al*., 2011). Normally, by synthesis of trichothecene mycotoxins, *Fg* is able to breach the rachis node and successfully infect the entire wheat head. The genes required for the production of these toxins are mostly found in a cluster (*TRI* genes) (Kimura *et al*., 2007) and are only expressed *in planta* or under special toxin-inducing conditions (Gardiner *et al*., 2009). Whether *Fg*Ebr1 is required for the production of these toxins is not known. It is also not known whether *Fg*Ebr1 regulates the *TRI* genes during wheat infection. In order to study the expression of *TRI* and other genes during wheat infection by wild type and Δ*ebr1*, we isolated RNA from inoculated wheat spikelets and used it for transcriptome analysis.

Genes involved in trichothecene biosynthesis were ≥ twofold less expressed in the mutant compared with wild type (Fig. S4). In total, we found that during infection, 100 genes were expressed at ≥ twofold lower levels in the Δ*ebr1* mutant compared with wild type and that 85 genes were expressed at ≥ twofold higher levels (Table S9). When we inspected the functional categories of genes that are expressed at a lower level in the Δ*ebr1* strain compared with wild type, we found the categories of amino acid metabolism (FunCat 01.01; $P = 3.30E-04$) and secondary metabolism (FunCat 01.20; $P + 7.47E-04$) over-represented and specifically the ones involved in regulation of amino acid metabolism (FunCat 01.01.13; $P + 0.005$), degradation and metabolism of tryptophan (FunCat 01.01.09.06.02; $P = 8.03E-05$), metabolism of the serine, glycine, cysteine and aromatic amino acids group (FunCat 01.01.09; $P = 4.86E-04$), biosynthesis and degradation of proline (FunCat 01.01.03.03.02; $P = 0.0012$), and of sesquiterpene metabolism (FunCat 01.06.06.05; $P = 0.0044$) (Table S10). Functional categorization of the genes that are expressed at higher levels in the Δ*ebr1* strain compared with wild type revealed that only the category of unclassified proteins was over-represented (FunCat 99; $P = 8.15E-04$) (Table S11). Surprisingly, we only found one gene to be down-regulated (FGSG_09596) and two genes up-regulated (FGSG_03969 and FGSG_04512) in both CM and *in planta* growth in the Δ*ebr1* compared with wild type. This suggests that Ebr1 regulates different gene sets in CM and *in planta*. FGSG_09596 encodes a hypothetical gene with no apparent conserved domains. FGSG_03969 encodes a cysteine-rich secreted protein and FGSG_04512 a predicted cation-transporting ATPase. Overall, the transcriptome results suggest that during infection of wheat, *Fg*Ebr1 affects the expression, directly or indirectly, of genes for toxin synthesis and amino acid metabolism.

To determine the levels of trichothecene produced by the different strains, wild-type PH-1, two independent Δ*ebr1* mutants and three complemented strains (see Experimental procedures) were used to inoculate wheat plants of the variety 'Norm'. Two weeks after inoculation, wheat heads were assessed for spread of disease symptoms, and inoculated spikelets were analysed for trichothecene toxin content. Separately, the wild type and the two Δ*ebr1* mutants were grown in toxin-inducing medium in order to determine the level of toxin production by the different strains *in vitro*. As mentioned earlier, no spread beyond the point of inoculation was observed for the deletion mutants on wheat heads (Fig. 7A). In contrast, the wild type and the complemented strain were able to spread and cause blighting symptoms in the inoculated and adjacent spikelets. When analysed for the presence of trichothecene mycotoxins, inoculated spikelets with all strains (wild type, the two Δ*ebr1* mutants or the three complements) contained trichothecene toxins. However, toxin levels were significantly lower in the two Δ*ebr1* mutants compared with wild type or complements (Student's *t*-test, $P \leq 0.05$). An average of approximately 370 parts per million (ppm) 15-ADON was found with wild type and the three complemented strains compared with an average 80 ppm (a reduction of approximately 78%) for the two Δ*ebr1* mutants (Fig. 7B). This is consistent with lower expression levels of the *TRI* genes found for the Δ*ebr1* mutant in the microarray experiment. *In vitro* toxin production was also significantly

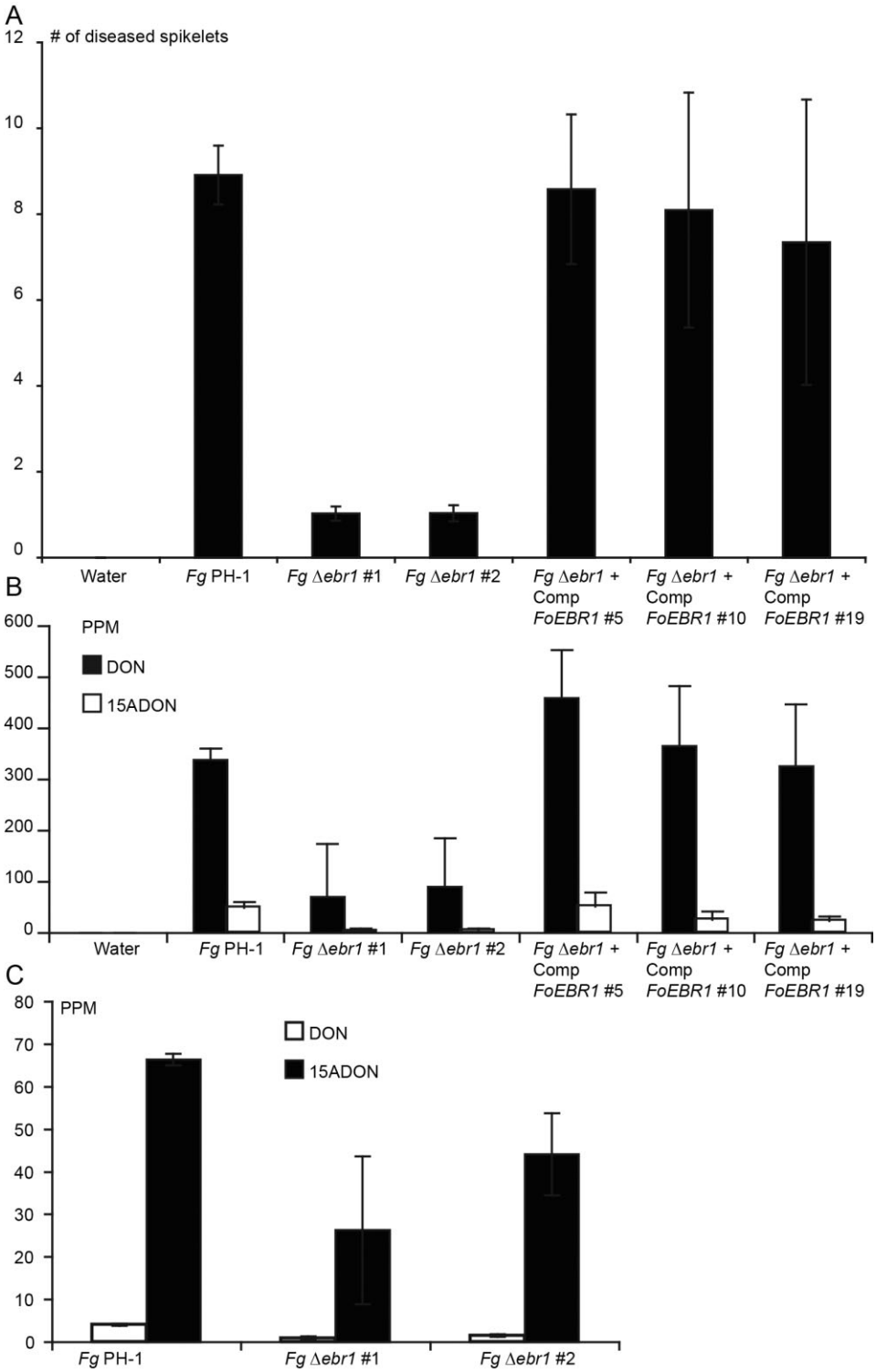

Fig. 7. *FgEBR1* is required for the full production of trichothecene toxins during growth *in planta* and in synthetic medium.
A. Average number of diseased spikelets of 30 plants after mock-inoculated with water, inoculated with wild type PH-1, with two independent *EBR1* deletion mutants or with three independent *FoEBR1* complemented transformants. Wheat heads were point inoculated and disease spread through adjacent spikelets was enumerated after 14 days. Error bars indicate standard deviation.
B. DON and 15-ADON toxin concentrations (parts per million – ppm) in the inoculated spikelet 14 days after inoculation with H_2O, wild-type PH-1, two independent *EBR1* deletion mutants or with three independent *FoEBR1* complemented transformants.
C. DON and 15-ADON toxin concentrations (parts per million – ppm) measured in putrescine medium after 1 week of growth with wild type or two independent *EBR1* deletion mutants.

lower for the two Δ*ebr1* mutants compared with wild type (Student's *t*-test, $P \leq 0.01$). In the mutants, about twofold lower toxin levels were found (Fig. 7C). This indicates that *Fg*Ebr1 is required for full trichothecene toxin production *in planta* as well as *in vitro*.

Using the microarray data, we also identified other gene clusters that are regulated by *Fg*Ebr1 in addition to the *TRI* gene cluster. For the *Fg* Δ*ebr1* strain growing in CM the aurofusarin biosynthesis genes (Malz *et al*., 2005), including polyketide synthase 12 (*PKS12*, FGSG_02324) (Hansen *et al*., 2012), are expressed to approximately 2- to 15-fold lower levels compared with wild type (Fig. S4B). During wheat infection, genes for aurofusarin synthesis were not expressed in wild type nor Δ*ebr1* mutant. Genes for butenolide synthesis, which also reside in a cluster (Harris *et al*., 2007), also are expressed at a lower level in the *Fg* Δ*ebr1* strain during wheat infection compared with wild type (Fig. S4C).

In *Fo*, no gene clusters for secondary metabolite synthesis appear to be affected by *Fo*Ebr1 during growth in CM (data not shown). However, *Fo*Ebr1 positively affects expression of two genes that encode non-ribosomal peptide synthases (NRPS) (Hansen *et al*., 2012): *NRPS2* (FOXG_06448) and *NRPS6* (FOXG_09785). These two genes are expressed in the microarray experiment to approximately threefold and eightfold lower levels in *Fo* Δ*ebr1* compared with wild type. Both genes are required for siderophore synthesis (Hansen *et al*., 2012) as is another gene (FOXG_06447), encoding ornithine-N5-oxygenase that is four times less expressed in *Fo* Δ*ebr1* compared with wild type (data not shown). Genes homologous to these three in *Fg* are not differentially expressed between wild type and *Fg* Δ*ebr1*, either during growth in CM or during spikelet infection. This suggests that in *Fo*, *EBR1* might positively regulate siderophore synthesis, while it does not seem to do so in *Fg*.

Discussion

Ebr1 affects the expression of genes involved in metabolism and virulence

Fungal-specific Zn_2Cys_6 TFs play pivotal roles in the life of fungi (MacPherson *et al*., 2006). *EBR1* is a gene encoding such a fungal-specific TF and seems to play a role in growth by regulating many genes involved in primary metabolism. Along with vegetative growth, *EBR1* also seems to play a role in sexual reproduction in *Fg* because the *Fg* Δ*ebr1* mutant is impaired in formation of normal perithecia. When grown on carrot agar to induce perithecium formation, mutants of this homothallic fungus show reduced radial growth compared with wild type. When the mycelium is induced for sexual reproduction by addition of Tween-60, just a few perithecia are formed in contrast with wild type that forms many perithecia (data not shown). While it is possible that Ebr1 directly regulates genes involved in perithecium formation, it is also conceivable that metabolic deficiencies of the mutants, as reflected in their reduced growth rate on complex media, account for the reduction in perithecium initiation.

During vegetative growth in CM, Ebr1 seems to regulate primary metabolism. Some of the genes that seemingly are regulated similarly by Ebr1 in both *Fg* and *Fol* are involved in primary metabolism, and the down-regulation of these genes might explain the growth defect of the mutants in both species as investigated in this study and previously (Zhao *et al*., 2011). *In planta*, *Fg*Ebr1 also controls the expression of the *TRI* genes responsible for the trichothecene toxin biosynthesis. Reduced *TRI* gene expression in Δ*ebr1* mutants may indicate direct positive regulation or could be explained by indirect effects such as feedback inhibition because of overall reduction in primary metabolism causing a depletion of toxin precursors and other secondary metabolites. Amino acid metabolism pathways in particular seem to be down-regulated in mutants during infection, which might indirectly account for the lower toxin production. Reduced trichothecene levels in Δ*ebr1* mutants almost certainly accounts in part for their reduced virulence towards wheat. However, whether the reduced toxin levels alone may explain the inability of mutants to spread through the rachis is unknown. Other important pathogenicity genes also may be reduced in expression in *Fg* Δ*ebr1* preventing the mutant from fully colonizing the wheat head.

FoEBR1 plays a smaller role in virulence compared to *FgEBR1*. The reduced pathogenicity of *Fo*Δ*ebr1* perhaps could be due to overall reduced hyphal growth as observed on agar plates. Also, the presence of the extra *EBR* genes might explain why the Δ*ebr1* strain retains a degree of pathogenicity. In wild-type *Fol* 4287, *EBR1* was predominantly expressed during the first 2 days of tomato root infection, and *EBR2* was predominantly expressed in the Δ*ebr1* strain. An analysis of total *EBR* expression in wild type and Δ*ebr1* strains during the first 2 days of tomato root infection revealed that overall transcript levels did not vary greatly (data not shown). This means that in the absence of *EBR1*, the *EBR* paralogues, and foremost *EBR2*, may compensate through higher expression and function to partially replace the missing *EBR1* during seedling infection.

We also found that biocontrol properties were affected in some but not all *Fo* Δ*ebr1* mutants. The reduction of biocontrol properties of these mutants is not so severe that it is completely unable to fend off the pathogenic strain *Foln*. Whether the growth characteristics essential for biocontrol properties and pathogenicity are related to the growth characteristics on agar plates is therefore difficult to address.

Recently, the transcriptome of wild-type PH-1 and a *Fg* Δ*ebr1* strain were compared in an RNAseq study that had the goal of improving the annotation of *Fg* genes (Zhao *et al*., 2013). This RNAseq study also showed that expression values of many genes differed between wild type and *Fg* Δ*ebr1* mutant, similar to our study. Comparing this RNAseq study to our results involving microarrays, however, is complicated due to differences in the experimental set-up and the fact that different *Fg* Δ*ebr1* mutants were used. Another difference was that the RNAseq study used RNA from strains growing in CM for 30 h versus 48 h in our study, and so it is possible that the strains were at different developmental stages during RNA sampling. The overlapping number of > twofold down-regulated genes in the *Fg* Δ*ebr1* strain compared with wild type for both studies is 123 out of the total of 941 (microarray experiment) or 1623 (RNAseq experiment). The overlapping number of genes > twofold up-regulated in the *Fg* Δ*ebr1* strain compared with wild type in both studies is 413 out of the total of 1308 (microarray experiment) or 3625 (RNAseq experiment) (data not shown). This overlap is rather small probably because of the biological differences discussed earlier and the greater sensitivity of the RNAseq approach to detect differential gene expression.

Presence of multiple EBR genes in Fo strains

Except for pathogenic *F. oxysporum* strains, *EBR1* is found only as a single copy gene in other fungi. Presence of *EBR1* is restricted to fungi belonging to the Pezizomycotina as determined by BLAST searches. In *Fol* so far, *EBR1* and four paralogues, *EBR2*, *3*, *4* and *5* have been found. But in other pathogenic *Fo* strains, additional sequence variants are likely present. Using CHEF electrophoresis and Southern hybridization, we have been able to determine the sequence diversity as well as locus diversity of *EBR* genes and demonstrated that in addition to the *EBR1* gene in the core genome, between one and four paralogues are present and located on small chromosomes in most pathogenic *F. oxysporum* strains. The expansion of *EBR* genes in pathogenic lineages may imply a contribution to virulence or niche specialization.

Other TF genes present in multiple copies may contribute to pathogenicity

From analysis of the genome sequence of *Fol* 4287, it became clear that the pool of putative TF genes is expanded in *Fol* compared with *Fg* or *F. verticillioides* with predicted TFs numbering 881, 716 and 683 respectively. In *Fol*, 119 out of the 881 genes are found in LS regions (Ma *et al*., 2010), of which 27 are of the Zn_2Cys_6 type. One such TF with a putative Zn_2Cys_6-domain is *FTF1*, which is found in multiple copies in *Fol* and in highly virulent strains of the bean pathogen *F. oxysporum* f. sp. *phaseoli*. In the bean pathogen, the genes are specifically expressed during early stages of host infection, which implies that this TF may regulate genes important for virulence or host colonization (Ramos *et al*., 2007). The multiple paralogues of *FTF1* found in *Fol* might be equally important for virulence (de Vega-Bartol *et al*., 2011). In *Fol* 4287, 11 paralogues of *FTF1* are present in LS regions: three on chromosome 14, one on chromosome 15, one on the LS region of chromosome 1, three on chromosome 6 and two on chromosome 3. The related gene *FTF2* (FOXG_09390) is present on core chromosome 9 (Table S12A). The exact role and target genes of Ftf1 in *F. oxysporum* are not known. A deletion of one copy in *F. oxysporum* f. sp. *phaseoli* has no effect on bean infection (de Vega-Bartol *et al*., 2011), but silencing efforts to study the effect of a down-regulation of the entire *FTF1* gene family are under investigation (J.J. de Vega and J.M. Diaz-Minguez, unpubl. data).

FOW2 (FOXG_06378, present on chromosome 2), a gene that also encodes a Zn_2Cys_6-domain TF, is required for infection of melon and tomato by *F. oxysporum* f. sp. *melonis* (*Fom*) and *Fol* respectively (Imazaki *et al*., 2007; Michielse *et al*., 2009a). Two paralogues are identified in *Fol*, and it is unknown whether paralogues exist in *Fom.* The two paralogues in *Fol* 4287 are located on repeated segments of chromosome 3 (FOXG_12458) and chromosome 6 (FOXG_14079). Deletion of *FOW2* in *Fom* results in complete loss of pathogenicity (Imazaki *et al*., 2007); however, two independent insertional mutants in *Fol* reduced pathogenicity to only about 50% of wild-type level (Michielse *et al*., 2009a). These insertions were in the 5′ region, which might explain the difference regarding plant infection compared with the complete ORF deletion of *FOW2* in *Fom*. However, also the presence of the two paralogues in *Fol* could explain this milder phenotype of mutants. In contrast with *EBR1*, homologues of *FOW2* and *FTF2* in *Fg* (FGSG_05309 and FGSG_05503 respectively) are not required for pathogenicity, although *FgFTF2* does play a role in ascospore formation and discharge (Son *et al*., 2011).

Some TF genes required for pathogenicity of *Fg* are expanded in *Fol* similar to *EBR1*. One such gene is FGSG_06651, encoding a basic-leucine zipper domain TF. The mutant deleted for this gene in *Fg* (Δ*GzbZIP010*) shows impaired growth, is completely avirulent, and produces no zearalenone or trichothecene toxins (Son *et al*., 2011). The closest *Fol* homologue and presumed orthologue FOXG_02290 is located on chromosome 5, and the 12, mostly partial, paralogues are found on chromosome 14 (3 genes), chromosome 3 (4 genes) and

chromosome 6 (5 genes) (Table S12B). Remarkably, one of the paralogues on chromosome 14, FOXG_14274, is located close to *EBR2* (FOXG_14277), and together, these genes are on a segment that is repeated on chromosome 3 and chromosome 6 where the other paralogues are closely linked to *EBR3* and *EBR4*.

Another TF gene expansion in *Fol* is related to FGSG_10517, encoding a C_2H_2-finger domain TF. A mutant deleted for this gene in *Fg* (*GzC_2H090*) shows many defects including poor growth on minimal medium, sterility, lack of conidiation, reduced trichothecene accumulation, enhanced zearalenone synthesis, and avirulence towards wheat (Son *et al*., 2011). In addition to the closest *Fol* homologue and presumed orthologue FOXG_04904 found on core chromosome 7, one paralogue is found on chromosome 14 (FOXG_14202), and three partial paralogues are found each on chromosome 3 and chromosome 6 (Table S12C). Interestingly, no paralogues of *EBR1*, *FTF2*, *FOW2* or paralogues of the TFs described earlier are present in *F. solani* f. sp. *pisi* (also known as *Nectria haematococca*), a pathogen of pea that also contains supernumerary chromosomes important for pathogenicity (VanEtten *et al*., 1994).

Why do pathogenic F. oxysporum *strains contain so many expanded TF gene families?*

What forces drive the expansion of TF genes on the supernumerary chromosomes in *F. oxysporum*? Is it possible that all these paralogues in some way contribute to virulence, host specificity or fitness on plants? *Fusarium oxysporum* strains can exchange small chromosomes via horizontal transfer, a process through which a non-pathogenic strain can transform into a pathogenic one (Ma *et al*., 2010). While the exchanged small chromosomes must contain genes that encode for pathogenicity, such as the *SIX* genes, it is unclear whether other genes on these chromosomes may have merely 'hitchhiked' to the other strain by virtue of being located on the same chromosome and may in fact be unrelated to pathogenicity. *EBR2*, for instance, might either be a virulence gene or a hitchhiker.

The mechanism for the expansion of genes in LS regions may involve transposons that are extremely numerous on supernumerary chromosomes. It has been suggested that transposons may play a role in effector gene diversification (Rep and Kistler, 2010) by the generation of repeated DNA segments, which in turn may accelerate evolution of these segments. Such repeat-facilitated effector diversification may be the raw material upon which selection occurs for better adaptations to new hosts. A result of this rapid duplication, divergence and selective adaptation may be the generation of repetitive segments without adaptive function. If this is true, then many repeated genes on the four supernumerary chromosomes of *Fol* 4287 may simply be by-products of genomic rearrangement, and extra genes such as *EBR2, EBR3* and *EBR4*, while tolerated in the genome, are not necessarily required for pathogenicity. This may be true for *EBR3* and *EBR4* that are located exclusively on these two large extra chromosomes (3 and 6) but contribute little to the *EBR* transcript pool, especially during seedling infection. Furthermore, *EBR3* and *EBR4* are not present in all pathogenic *Fol* strains, which also suggests they have little importance to pathogenicity.

In contrast, *EBR2* is present in all pathogenic *Fol* strains probably on small supernumerary chromosomes. However, *EBR2* does not contribute much to the mRNA pool in *Fol* 4287 during the first 50 h after inoculation, although still its expression level is greater than that of *EBR3* and *EBR4*. Its contribution to the total transcript pool becomes larger later in infection, even though transcripts of *EBR1* remain most abundant. Unlike with *FTF1* in *F. oxysporum* f. sp. *phaseoli*, no significant rise in expression of *EBR2–4* occurs during the first 2 days of infection. The expression levels of the *EBR* genes therefore do not support the idea that gene family expansion is related to importance in infection and host colonization. Unfortunately, we were unable to delete *EBR2* and so we could not assess the effect of the complete elimination of the *EBR* gene family in a pathogenic *Fol* strain. Alternative methods for silencing of *EBR* gene transcript may help to clarify their role during infection. Also chromatin immunoprecipitation followed by DNA sequencing (ChIP-Seq) using Ebr1 or Ebr2 as baits may be informative to reveal whether they regulate different or similar sets of target genes.

Experimental procedures

Strains, plants and growth conditions

The fungal isolates used in this study are the sequenced strains of *Fg* PH-1 and *F. oxysporum* strains listed in Tables 1–3. All fungal strains were kept at −80° and revitalized on potato dextrose broth plus agar (PDB and Bacto agar, Difco, Franklin Lakes, NJ, USA). *Fg* strains were grown for 5 days in carboxymethylcellulose medium and *F. oxysporum* in rich CM for macroconidia and microconidia production respectively. *Agrobacterium tumefaciens* EHA105 (Hood *et al*., 1993),used for *Agrobacterium*-mediated transformations, was grown in LB containing 20 μg ml^{-1} rifampicin at 28°C.

The wheat varieties 'Norm' and 'Bobwhite', and the wilt susceptible tomato variety 'Moneymaker' were used for plant infection studies. Wheat pathogenicity assays were performed with cultivar 'Norm' using point inoculation (Goswami and Kistler, 2005) and were scored 2 weeks after inoculation by counting the number of symptomatic spikelets. Wheat infections used for microarray studies were performed with cultivar 'Bobwhite' using point inoculations of 10 spikelets of each head. At 72 hpi, anthers were removed, and the infected

spikelets were detached from the rachis, collected and frozen until RNA processing (Seong *et al*., 2009). Tomato infections were performed with 10-day-old seedlings that were inoculated using the root dip method, and disease was scored as described previously (Michielse *et al*., 2009b).

Inoculum preparation and biocontrol assay

Inocula were prepared as described before (Michielse *et al*., 2009b). A heat-treated (100°C for 1 h) silty-loam soil from Dijon [35.1% clay, 47% loam, 15.1% sand, and 1.22% organic C (pH = 6.9)] was added to module trays containing 96 wells each of 50 ml. To prevent contamination between treatments, only every second row of wells was filled with soil. The soil in each well was inoculated with 5 ml of conidia suspension. The concentration of the conidia in suspensions were adjusted to obtain the following inoculum densities: 1×10^3 conidia per ml of soil for the pathogenic strain Foln3 and 1×10^5 conidia per ml of soil for the others strains. The soil surface was covered with a thin layer of calcinated clay granules (Oil Dri Chem-Sorb, Brenntag Bourgogne, Montchanin, France), and three seeds of flax, cv. Opaline, were sown in each pot. A thin layer of Chem-Sorb was used to cover the seeds. Plants were grown in a growth chamber in the first 2 weeks; the growing conditions were 8 h 15°C dark/16 h 17°C light, with a light intensity of 33 $\mu E\ m^{-2}\ s^{-1}$. The plants were thinned to one plant per pot, and from week 3, the temperature was kept at 22°C dark/25°C light. There were three replicates of 16 individual plants per treatment randomly arranged. Plants were watered every day, and once every week, water was replaced by a 500-fold dilution of a commercial nutrient stock solution (Hydrodrokani AO, Hydro Agri, Nanterre, France). Plants showing characteristic symptoms of yellowing were recorded twice a week and removed. To compare the ability of strains to induce disease or, on the contrary, to protect the plant against wilt, ANOVA was performed on AUDPCs followed by Newman and Keuls test at the probability of 95%.

For the Biolog FF assay (Biolog FF plates™), each well was filled with 10^4 conidia in 150 µl. Time point zero was taken after 2 h on a spectrophotometer at 600 nm, when the lyophilized carbon sources were dissolved. Further measurements were made in duplicate at time points 24, 48, 72 and 96 h after inoculation.

Construction of gene replacement and complementation constructs

In order to generate deletion constructs of *FgEBR1*, PCR was used to amplify the upstream and downstream flanking sequences (approximately 2000 bp) of *FgEBR1* gene using primers 1 and 2, and 3 and 4 (Table S13). PCR products were ligated into plasmid pPK2*hphgfp* (Michielse *et al*., 2009a) after both product and plasmid were digested using the appropriate restriction enzymes. The upstream flanks of *EBR1* were cut with *Hind*III and *Xba*I and the downstream flanks with *Kpn*I and *Pac*I. First, the upstream flank was ligated into the plasmid and then the downstream flank. In order to generate deletion constructs of *FoEBR1*, PCR was used to amplify the upstream and downstream sequences (approximately 1000 bp) of each gene using primers 5 and 6, and 7 and 8 (Table S13). PCR products were ligated into plasmid pPK2*hphgfp* (Michielse *et al*., 2009a) as described for *FgEBR1*.

A *FoEBR1* complementation construct was generated in two pieces using PCR and primers 9 and 10, and 11 and 12 (Table S13). The two pieces were ligated in pGEMT-easy (Promega, Madison, WI, USA) and sequenced. Correct products were cut with *Stu*I and *Sac*II, and *Sac*II and *Xba*I for the first half and the second half of the gene respectively. Using three-point ligation, the products were ligated into plasmid pRW1p (Houterman *et al*., 2008), which was cut using enzymes *Stu*I and *Xba*I obtaining pRW1pEBR1Comp. For the three different truncated versions, the terminator including the stop-codon of *EBR1* was amplified using PCR with primers containing linkers with *Xba*I, *Pst*I or *Nsi*I sites (primers 12–15, Table S13). These terminator fragments were sequenced and cut with the enzyme in the linker and with *Xba*I. Using ligation, the *Xba*I-*Xba*I terminator fragment was ligated into plasmid pRW1p cut with *Xba*I, obtaining pRW1pEBR1*Xba*I. Using three-point ligation, the *Pst*I-*Xba*I terminator and *EBR1 Xba*I-*Pst*I or *Nsi*I-*Xba*I terminator fragment and *EBR1 Xba*I-*Nsi*I fragment were ligated into plasmid pRW1p cut with *Xba*I obtaining pRW1pEBR1*Pst*I and pRW1pEBR1*Nsi*I respectively. To obtain the *EBR2* complementation constructs, the *EBR2* ORF with upstream and downstream regions was amplified in two pieces using PCR with primers 16 and 17, and 18 and 19 (Table S13). The products were ligated in pGEMT-easy and sequenced. The first half was cut from pGEMT-easy using *Hin*dIII and the second half was cut using *Hin*dIII and *Spe*I. The second half was first ligated in pRW1p, which was cut with *Hin*dIII and *Xba*I, and subsequently the first half was ligated in the vector in the *Hin*dIII site, obtaining pRW1pEBR2Comp.

To create a construct with the promoter sequence of *EBR1 5′* to the coding sequence of *EBR2*, the promoter sequence of *EBR1* was amplified using PCR with primers 20 and 21 (Table S13), and the N-terminus of *EBR2* was amplified using PCR with primers 22 and 23 (Table S13), and ligated into pGEMT-easy for sequencing. The promoter product was cut with *Stu*I and *Spe*I, and the N-terminal amplicon digested with *Asc*I and *Spe*I. Using three-point ligation, the products were ligated into plasmid pRW1EBR2Comp, which was cut using enzymes *Pme*I and *Asc*I.

To complement one of the *EBR1* deletion mutants of *Fg*, we used the same plasmid with the complete ORF of *FoEBR1* plus 1 kb upstream that we used to complement the *Fo*Δ*ebr1* strain, pRW1pEBR1Comp. To enable selection on genetecin, we cloned the neomycin resistance cassette into the pRW1pEBR1Comp plasmid. This neomycin cassette was previously cut from pRW1p*FGP1*neo (Jonkers *et al*., 2012) using the flanking *Eco*RI and *Bsr*GI sites and ligated into plasmid pRW1pEBR1Comp cut with the same enzymes. Using this approach, we obtained three independent complementation mutants as verified by PCR (data not shown).

Fungal transformations

Agrobacterium-mediated transformation used for *F. oxysporum* and *F. graminearum* was performed as described previously (Takken *et al*., 2004; Jonkers *et al*., 2012). For deletion strains, transformants were checked by PCR using a primer that anneals to a region outside the recombination

locus of the gene and a primer that anneals to a region of the deletion *HPH* cassette (data not shown). At least two independent deletion mutants or ectopic mutants were obtained. All deletion mutants showed similar phenotypes. Complementation transformants were checked by PCR for presence of the desired inserted construct (data not shown). Strains containing the appropriate-sized PCR amplicons were used. At least three independent complementation mutants were obtained for each construct. All complementation mutants showed similar phenotypes on agar plates.

Trichothecene analysis

In vitro and *in planta* trichothecene toxin analysis were performed as described previously (Jonkers *et al*., 2012). In short, for the *in vitro* analysis, conidia (1×10^4 conidia ml^{-1}) of each strain were inoculated in six wells containing 2 ml of putrescine medium (30 g l^{-1} sucrose, 1 g l^{-1} KH_2PO_4, 0.5 g l^{-1} $MgSO_4$, 0.5 g l^{-1} KCl, 0.8 g l^{-1} putrescine, 2 ml l^{-1} $FeSO_4*H_2O$ solution (5 mg ml^{-1}) and 200 µl trace elements (50 g l^{-1} citrate, 50 g l^{-1} $ZnSO_4*7H_2O$, 2.5 g l^{-1} $CuSO_4*5H_2O$, 0.5 g l^{-1} H_3BO_3, 0.5 g l^{-1} $NaMoO_4*2H_2O$, 0.5 g l^{-1} $MnSO_4*H_2O$) and grown for 1 week in the dark at 25°C. For each sample, the filtrate was collected by passing it through one layer of miracloth, and 250 µl of culture filtrate was placed in a glass vial and lyophilized. Analysis of trichothecene content of samples from plants was performed by placing the spikelet 2 weeks after inoculation in a glass vial. Determination of DON, 3-ADON and 15-ADON concentration per unit mass in the vials was determined as described earlier (Goswami and Kistler, 2005).

Southern hybridization and CHEF electrophoresis

For Southern hybridization analysis, DNA was extracted using the CTAB (cetyl trimethylammonium bromide) protocol (Rosewich *et al*., 1999), and 1–2 µg DNA was used for restriction and loaded for gel electrophoresis. Transfer of DNA to HyBond N+ (GE Health Care, Pittsburgh, PA, USA) was performed using standard alkaline procedures according to the manufacturer's protocol. Probes for *EBR1* were amplified by PCR using primers 24 and 25. (Table S13). Probe hybridization and detection were performed using an AlkPhos kit and CDP-Star chemiluminescent solution (GE Health Care) according to the manufacturer's protocol. Images were obtained using the Carestream Image Station 4000MM Pro (Rochester, NY, USA).

CHEF electrophoresis was performed as described previously (Ma *et al*., 2010). In short, plugs containing 4×10^8 ml^{-1} protoplasts were loaded on a CHEF gel [1% Fastlane agarose (FMC, Philadelphia, PA, USA) in 0.5 × TBE] and ran for 255 h using switch times between 1200 and 4800 s at 1.8 V cm^{-1} (= 60 Volts). Chromosomes of *S. pombe* were used as molecular size markers (Bio-Rad, Philadelphia, PA, USA). Subsequent Southern blotting and detection was performed as described above.

EBR ratio determination by PCR and restriction enzyme digestion

We harvested fresh conidia of *Fol* 4287 and the Δ*ebr1* mutant and used them to inoculated 50 ml CM (1×10^4 spores ml^{-1}) in triplicate or tomato seedlings in 10 ml tap water containing 1×10^7 spores ml^{-1} in duplo. Samples for RNA extraction (see discussion later) were collected from CM cultures after 48 h and from plants after three through 50 h. cDNA was subsequently produced from the RNA and used to amplify the *EBR* products. For each *EBR* paralogue, the same region used for Southern hybridization was amplified using genomic DNA or cDNA with primers 24 and 25 (Table S13). The primer sequences for each paralogue are identical, and the product size is exactly the same; therefore, we assume that the PCR efficiency should also be the same for each paralogue. The amplified PCR products were extracted from the electrophoresis gel, ligated into the pGEM-T easy vector (Promega) according to the manufacturer's protocol and transformed to chemically competent *E. coli* cells. Cells of individual colonies were diluted in water (5 µl cells and 50 µl water), and 1 µl of this mixture was used in a PCR reaction. The primers [M13F and M13R (26 and 27); Table S13] align approximately 100 bp from the insertion site. The PCR product is approximately 800 bp when an *EBR* insert is present and 200 bp when not.

From each sample, at least 96 colonies were screened and subsequently digested. The amplified product of *EBR* differs for each paralogue in such a way that a unique restriction site is present for each of the *EBR* paralogues (Fig. 6A). To determine whether *EBR2* was present, we cut the PCR product with *Bam*HI, which cuts specifically in *EBR2*. A positive *EBR2* product gives two bands of about 250 and 550 bp. A negative *EBR2* product gives one band of about 800 bp. To determine whether *EBR3* was present, we cut the PCR product with *Sal*I, which cuts specifically in *EBR3* and in the amplified piece of the pGEMT-vector. A positive *EBR3* product gives three bands of about 100, 200 and 500 bp, or 100, 100 and 600 bp depending on the orientation. A negative *EBR3* product gives two bands of about 100 and 700 bp. To determine whether *EBR4* was present, we cut the PCR product with *Hin*dIII, which cuts specifically in *EBR4*. A positive *EBR4* product gives two bands of about 250 and 550 bp. A negative *EBR4* product gives one band of about 800 bp. When a product proves to be negative for all three: *EBR2*, *EBR3* or *EBR4* but still has an insert it is classified as *EBR1*.

RNA extraction and reverse transcriptase-qPCR

RNA was extracted using Trizol (Invitrogen, Grand Island, NY, USA) according to manufacturer's protocol with an alternative precipitation step using one-half volume of isopropanol and a one-half volume of salt solution (0.8 M sodium citrate, 1.2 M NaCl). RNA was extracted from mycelium growing in 50 ml CM (1×10^4 spores ml^{-1}) for 48 h in the dark at 25°C with shaking at 150 r.p.m. Mycelium from cultures was harvested by filtration over one or two layers of miracloth, washed with water and frozen in liquid nitrogen. Mycelium was then lyophilized and ground in a mortar and pestle prior to Trizol extraction. RNA also was isolated from inoculated wheat spikelets and inoculated tomato roots, which were harvested, frozen in liquid nitrogen, and ground in a mortar and pestle prior to Trizol extraction.

RNA clean-up was done using the RNeasy Mini Kit (Qiagen, Valencia, CA, USA) prior to reverse transcriptase or microarray labelling. RNA labelling reactions were performed

according to the standard Affymetrix protocols. The CM and wheat infection samples were hybridized to an updated Affymetrix nine fungal plant pathogen GeneChip (http://www.plexdb.org). Hybridizations were performed at the BioMedical Genomics Center of the University of Minnesota.

RNA (2 μg) was treated with DNase (Invitrogen) and used for reverse transcriptase-PCR with SuperScript III Reverse Transcriptase (Invitrogen) according to manufacturer's protocol. The cDNA obtained by different methods was used as template to determine the ratios as described earlier or sequenced (Sanger sequencing) to determine the ORF start site and intron positions in the different *EBR* paralogues.

Microarray data analysis

Data files (.CEL) were imported in Refiner 5.3 software (Genedata Expressionist, Lexington, MA, USA) and robust multi-array average (RMA) preprocessing was applied. Signal values (*P*-value 0.04) obtained in the Analyst software (Expressionist) were normalized to the median. Fold-expression filters were applied as described in the results. Probe sets on the nine fungal plant pathogen genome array GeneChips were designed based on the FG3 assembly for *Fg* and the FO2 assembly for *F. oxysporum* [Fusarium Comparative Sequencing Project, Broad Institute of Harvard and MIT (http://www.broadinstitute.org/)]. For the experiments with both *Fg* and *F. oxysporum* grown in CM, a *F. oxysporum* orthologue was queried by BLAST (Altschul *et al*., 1997) for every *Fg* gene showing altered expression. In order to establish whether a gene was conserved in both *F. oxysporum* and *Fg*, we searched for the respective orthologues using BLAST, and a hit was considered a full orthologue at a bit score of > 200. Data and CEL files for microarray experiments are available at http://www.plexdb.org (Dash *et al*., 2012) under accession numbers NF8 and NF9 (growth on CM) and NF10 (wheat infection).

Acknowledgements

The authors thank Liane Gale for preparations of plugs for CHEF electrophoresis. Aaron Becker from the BioMedical Genomics Center at the University of Minnesota is thanked for processing the microarray chips. The Minnesota Supercomputing Institute is kindly acknowledged for computing resources and support. Yanhong Dong from the Department of Plant Pathology at the University of Minnesota is kindly thanked for performing the toxin analysis. This project was made possible by the United States Department of Agriculture (USDA), National Institute of Food and Agriculture (NIFA) and Agriculture and Food Research Initiative (AFRI) awards 2008–35604-18800 and 2010–65108-20642.

References

Alabouvette, C., Olivain, C., Migheli, Q., and Steinberg, C. (2009) Microbiological control of soil-borne phytopathogenic fungi with special emphasis on wilt-inducing *Fusarium oxysporum*. *New Phytol* **184:** 529–544.

Altschul, S.F., Madden, T.L., Schaffer, A.A., Zhang, J., Zhang, Z., Miller, W., and Lipman, D.J. (1997) Gapped BLAST and PSI-BLAST: a new generation of protein database search programs. *Nucleic Acids Res* **25:** 3389–3402.

Cai, G., Rosewich Gale, L., Schneider, R.W., Kistler, H.C., Davis, R.M., Elias, K.S., and Miyao, E.M. (2003) Origin of race 3 of *Fusarium oxysporum* f. sp. *lycopersici* at a single site in California. *Phytopathology* **93:** 1014–1022.

Coleman, J.J., Rounsley, S.D., Rodriguez-Carres, M., Kuo, A., Wasmann, C.C., Grimwood, J., *et al*. (2009) The genome of *Nectria haematococca*: contribution of supernumerary chromosomes to gene expansion. *PLoS Genet* **5:** e1000618.

Cuomo, C.A., Guldener, U., Xu, J.R., Trail, F., Turgeon, B.G., Di Pietro, A., *et al*. (2007) The *Fusarium graminearum* genome reveals a link between localized polymorphism and pathogen specialization. *Science* **317:** 1400–1402.

Dash, S., Van Hemert, J., Hong, L., Wise, R.P., and Dickerson, J.A. (2012) PLEXdb: gene expression resources for plants and plant pathogens. *Nucleic Acids Res* **40:** D1194–D1201.

Di Pietro, A., Madrid, M.P., Caracuel, Z., Delgado-Jarana, J., and Roncero, M.I.G. (2003) *Fusarium oxysporum*: exploring the molecular arsenal of a vascular wilt fungus. *Mol Plant Pathol* **4:** 315–325.

Dufresne, M., van der Lee, T., M'Barek, S.B., Xu, X., Zhang, X., Liu, T., *et al*. (2008) Transposon-tagging identifies novel pathogenicity genes in *Fusarium graminearum*. *Fungal Genet Biol* **45:** 1552–1561.

Fourie, G., Steenkamp, E.T., Gordon, T.R., and Viljoen, A. (2009) Evolutionary relationships among the vegetative compatibility groups of *Fusarium oxysporum* f.sp. cubense. *Appl Environ Microbiol* **75:** 4770–4781.

Fravel, D., Olivain, C., and Alabouvette, C. (2003) *Fusarium oxysporum* and its biocontrol. *New Phytol* **157:** 493–502.

Gale, L.R., Katan, T., and Kistler, H.C. (2003) The probable center of origin of *Fusarium oxysporum* f. sp. *lycopersici* VCG 0033. *Plant Dis* **87:** 1433–1438.

Gardiner, D.M., Kazan, K., and Manners, J.M. (2009) Nutrient profiling reveals potent inducers of trichothecene biosynthesis in *Fusarium graminearum*. *Fungal Genet Biol* **46:** 604–613.

Goswami, R.S., and Kistler, H.C. (2004) Heading for disaster: *Fusarium graminearum* on cereal crops. *Mol Plant Pathol* **5:** 515–525.

Goswami, R.S., and Kistler, H.C. (2005) Pathogenicity and in planta mycotoxin accumulation among members of the *Fusarium graminearum* species complex on wheat and rice. *Phytopathology* **95:** 1397–1404.

Hansen, F.T., Sørensen, J.L., Giese, H., Sondergaard, T.E., and Frandsen, R.J.N. (2012) Quick guide to polyketide synthase and nonribosomal synthetase genes in *Fusarium*. *Int J Food Microbiol* **155:** 128–136.

Harris, L.J., Alexander, N.J., Saparno, A., Blackwell, B., McCormick, S.P., Desjardins, A.E., *et al*. (2007) A novel gene cluster in *Fusarium graminearum* contains a gene that contributes to butenolide synthesis. *Fungal Genet Biol* **44:** 293–306.

Hood, E.E., Gelvin, S.B., Melchers, L.S., and Hoekema, A. (1993) New *Agrobacterium* helper plasmids for gene transfer to plants. *Transgenic Res* **2:** 208–218.

Houterman, P.M., Speijer, D., Dekker, H.L., de Koster, C.G., Cornelissen, B.J., and Rep, M. (2007) The mixed xylem

sap proteome of *Fusarium oxysporum*-infected tomato plants. *Mol Plant Pathol* **8:** 215–221.

Houterman, P.M., Cornelissen, B.J.C., and Rep, M. (2008) Suppression of plant resistance gene-based immunity by a fungal effector. *PLoS Pathog* **4:** e1000061.

Houterman, P.M., Ma, L., van Ooijen, G., de Vroomen, M.J., Cornelissen, B.J.C., Takken, F.L.W., and Rep, M. (2009) The effector protein Avr2 of the xylem colonizing fungus *Fusarium oxysporum* activates the tomato resistance protein I-2 intracellularly. *Plant J* **58:** 970–978.

Imazaki, I., Kurahashi, M., Iida, Y., and Tsuge, T. (2007) Fow2, a Zn(II)2Cys6-type transcription regulator, controls plant infection of the vascular wilt fungus *Fusarium oxysporum*. *Mol Microbiol* **63:** 737–753.

Jeon, J., Park, S.Y., Chi, M.H., Choi, J., Park, J., Rho, H.S., *et al*. (2007) Genome-wide functional analysis of pathogenicity genes in the rice blast fungus. *Nat Genet* **39:** 561–565.

Jonkers, W., Dong, Y., Broz, K., and Kistler, H.C. (2012) The Wor1-like protein Fgp1 regulates pathogenicity, toxin synthesis and reproduction in the phytopathogenic fungus *Fusarium graminearum*. *PLoS Pathog* **8:** e1002724.

Khalil, S., and Alsanius, B.W. (2009) Utilisation of carbon sources by *Pythium*, *Phytophthora* and *Fusarium* species as determined by Biolog microplate assay. *Open Microbiol J* **3:** 9–14.

Kimura, M., Tokai, T., Takahashi-Ando, N., Ohsato, S., and Fujimura, M. (2007) Molecular and genetic studies of Fusarium trichothecene biosynthesis: pathways, genes, and evolution. *Biosci Biotechnol Biochem* **71:** 2105–2123.

Kistler, H.C., Alabouvette, C., Baayen, R.P., Bentley, S., Brayford, D., Coddington, A., *et al*. (1998) Systematic numbering of vegetative compatibility groups in the plant pathogenic fungus *Fusarium oxysporum*. *Phytopathology* **88:** 30–32.

Kraulis, P.J., Raine, A.R., Gadhavi, P.L., and Laue, E.D. (1992) Structure of the DNA-binding domain of zinc GAL4. *Nature* **356:** 448–450.

Lievens, B., Houterman, P.M., and Rep, M. (2009) Effector gene screening allows unambiguous identification of *Fusarium oxysporum* f. sp. *lycopersici* races and discrimination from other formae speciales. *FEMS Microbiol Lett* **300:** 201–215.

Ma, L.-J., van der Does, H.C., Borkovich, K.A., Coleman, J.J., Daboussi, M.-J., Di Pietro, A., *et al*. (2010) Comparative genomics reveals mobile pathogenicity chromosomes in *Fusarium*. *Nature* **464:** 367–373.

MacPherson, S., Larochelle, M., and Turcotte, B. (2006) A fungal family of transcriptional regulators: the zinc cluster proteins. *Microbiol Mol Biol Rev* **70:** 583–604.

Malz, S., Grell, M.N., Thrane, C., Maier, F.J., Rosager, P., Felk, A., *et al*. (2005) Identification of a gene cluster responsible for the biosynthesis of aurofusarin in the *Fusarium graminearum* species complex. *Fungal Genet Biol* **42:** 420–433.

Marlatt, M.L., Correll, J.C., Kaufmann, P., and Cooper, P.E. (1996) Two genetically distinct populations of *Fusarium oxysporum* f. sp. *lycopersici* race 3 in the United States. *Plant Dis* **80:** 1336–1342.

Mes, J.J., Weststeijn, E.A., Herlaar, F., Lambalk, J.J.M., Wijbrandi, J., Haring, M.A., and Cornelissen, B.J.C. (1999) Biological and molecular characterization of *Fusarium oxysporum* f. sp. *lycopersici* divides race 1 isolates into separate virulence groups. *Phytopathology* **89:** 156–160.

Michielse, C.B., and Rep, M. (2009) Pathogen profile update: *Fusarium oxysporum*. *Mol Plant Pathol* **10:** 311–324.

Michielse, C.B., van Wijk, R., Reijnen, L., Cornelissen, B.J., and Rep, M. (2009a) Insight into the molecular requirements for pathogenicity of *Fusarium oxysporum* f. sp. *lycopersici* through large-scale insertional mutagenesis. *Genome Biol* **10:** R4.

Michielse, C.B., van Wijk, R., Reijnen, L., Manders, E.M., Boas, S., Olivain, C., *et al*. (2009b) The nuclear protein Sge1 of *Fusarium oxysporum* is required for parasitic growth. *PLoS Pathog* **5:** e1000637.

O'Donnell, K., Sutton, D.A., Rinaldi, M.G., Magnon, K.C., Cox, P.A., Revankar, S.G., *et al*. (2004) Genetic diversity of human pathogenic members of the *Fusarium oxysporum* complex inferred from multilocus DNA sequence data and amplified fragment length polymorphism analyses: evidence for the recent dispersion of a geographically widespread clonal lineage and nosocomial origin. *J Clin Microbiol* **42:** 5109–5120.

Ramos, B., Alves-Santos, F.M., García-Sánchez, M.A., Martín-Rodrigues, N., Eslava, A.P., and Díaz-Mínguez, J.M. (2007) The gene coding for a new transcription factor (*ftf1*) of *Fusarium oxysporum* is only expressed during infection of common bean. *Fungal Genet Biol* **44:** 864–876.

Rep, M., and Kistler, H.C. (2010) The genomic organization of plant pathogenicity in *Fusarium* species. *Curr Opin Plant Biol* **13:** 420–426.

Rep, M., van der Does, H.C., Meijer, M., van Wijk, R., Houterman, P.M., Dekker, H.L., *et al*. (2004) A small, cysteine-rich protein secreted by *Fusarium oxysporum* during colonization of xylem vessels is required for I-3-mediated resistance in tomato. *Mol Microbiol* **53:** 1373–1383.

Rosewich, U.L., Pettway, R.E., Katan, T., and Kistler, H.C. (1999) Population genetic analysis corroborates dispersal of *Fusarium oxysporum* f. sp. *radicis-lycopersici* from Florida to Europe. *Phytopathology* **89:** 623–630.

Ruepp, A., Zollner, A., Maier, D., Albermann, K., Hani, J., Mokrejs, M., *et al*. (2004) The FunCat, a functional annotation scheme for systematic classification of proteins from whole genomes. *Nucleic Acids Res* **32:** 5539–5545.

Seong, K.Y., Pasquali, M., Zhou, X., Song, J., Hilburn, K., McCormick, S., *et al*. (2009) Global gene regulation by *Fusarium* transcription factors *Tri6* and *Tri10* reveals adaptations for toxin biosynthesis. *Mol Microbiol* **72:** 354–367.

Shinohara, M.L., Correa, A., Bell-Pedersen, D., Dunlap, J.C., and Loros, J.J. (2002) *Neurospora* clock-controlled gene 9 (ccg-9) encodes trehalose synthase: circadian regulation of stress responses and development. *Eukaryot Cell* **1:** 33–43.

Slattery, M.G., Liko, D., and Heideman, W. (2006) The function and properties of the Azf1 transcriptional regulator change with growth conditions in *Saccharomyces cerevisiae*. *Eukaryot Cell* **5:** 313–320.

Son, H., Seo, Y.S., Min, K., Park, A.R., Lee, J., Jin, J.M., *et al*. (2011) A phenome-based functional analysis of transcrip-

tion factors in the cereal head blight fungus, *Fusarium graminearum*. *PLoS Pathog* **7:** e1002310.
Takken, F.L., Van Wijk, R., Michielse, C.B., Houterman, P.M., Ram, A.F., and Cornelissen, B.J. (2004) A one-step method to convert vectors into binary vectors suited for *Agrobacterium*-mediated transformation. *Curr Genet* **45:** 242–248.
Thatcher, L.F., Gardiner, D.M., Kazan, K., and Manners, J.M. (2012) A highly conserved effector in *Fusarium oxysporum* is required for full virulence on Arabidopsis. *Mol Plant Microbe Interact* **25:** 180–190.
VanEtten, H., Funnell-Baerg, D., Wasmann, C., and McCluskey, K. (1994) Location of pathogenicity genes on dispensable chromosomes in *Nectria haematococca* MPVI. *Antonie Van Leeuwenhoek* **65:** 263–267.
de Vega-Bartol, J.J., Martin-Dominguez, R., Ramos, B., Garcia-Sanchez, M.A., and Diaz-Minguez, J.M. (2011) New virulence groups in *Fusarium oxysporum* f. sp. *phaseoli*: the expression of the gene coding for the transcription factor ftf1 correlates with virulence. *Phytopathology* **101:** 470–479.
Zhao, C., Waalwijk, C., de Wit, P.J., van der Lee, T., and Tang, D. (2011) EBR1, a novel Zn(2)Cys(6) transcription factor, affects virulence and apical dominance of the hyphal tip in *Fusarium graminearum*. *Mol Plant Microbe Interact* **24:** 1407–1418.
Zhao, C., Waalwijk, C., de Wit, P.J., Tang, D., and van der Lee, T. (2013) RNA-Seq analysis reveals new gene models and alternative splicing in the fungal pathogen *Fusarium graminearum*. *BMC Genomics* **14:** 21.

Supporting information

Additional may be found in the online version of this article at the publisher's web-site:

Fig. S1. Antonie Van Leeuwenhoek's divergence in the 5′ upstream regions of the four *EBR* paralogues and alignment of the full protein sequences of the four *Fo*Ebr proteins to *Fg*Ebr1.
A. Schematic overview of DNA alignment results of the 5′ upstream regions of the four *EBR* genes (1000 base pairs upstream of predicted start codon). The gray bar of *EBR1* indicates no DNA alignment observed with any of the other *EBR* 5′ upstream regions. The black portions of the bars of *EBR2*, *EBR3* and *EBR4* indicate strong DNA alignment observed between their 5′ upstream regions. The white blocks in between represent gaps in the alignment. The diagonal striped bar indicates substantial loss of DNA alignment observed.
B. Protein sequence alignment of five *Fusarium* Ebr proteins: *Fg*Ebr1 (FGSG_10057) from *F. graminearum*, *Fo*Ebr1, *Fo*Ebr2, *Fo*Ebr3 and *Fo*Ebr4 from *F. oxysporum*. Conserved and similar residues are shaded grey. The full black boxed residues form the Zn_2Cys_6-domain and the dashed black boxed residues the fungal specific transcription factor domain. The numbers 1, 2 and 3 represent the position of the stop codons placed in the three truncated mutants as explained in the text. The protein alignment was created using MacVector version 10.6.0.
Fig. S2. The *FoEBR1* deletion mutant is impaired in certain carbon source utilization. Biolog FF MicroPlates containing in each well a different carbon source were used to analyse carbon utilization of the wild type and Δ*ebr1* mutant. A conidial suspension (10^4 conidia in 150 μl) of the wild type *Fol* 4287 or the two independent Δ*ebr1* strains was inoculated in each well and incubated at 25°C for 4 days, and each strain was analysed in duplo. The absorbance of each well at 600 nm was measured with a microtitre plate reader (Packard SpectraCount) at each day of incubation. Curves representing the sum of absorbance in all wells are produced for the *Fol* 4287 and the two independent Δ*ebr1* strains, and are shown in the inlet. The black curve = *Fol* 4287, the grey curve = Δ*ebr1* #1 and the dashed black curve = Δ*ebr1* #2. The ratios of absorbance of each well after 4 days were calculated by dividing the average measured values of the mutant strains by those of the wild-type strain. Only values higher than 2 or lower than 0.5 were marked (above and below the black lines) as carbon sources in which the Δ*ebr1* strain appeared to display a different growth rate than the wild-type strain (arrow pointing downwards = less growth of Δ*ebr1* compared with wild type, arrow pointing upwards = better growth of Δ*ebr1* compared with wild type). The numbers of each column represent the carbon sources as given in Table S1.
Fig. S3. The Δ*ebr1* and its parental strain exhibit biocontrol activity on flax. Histograms showing the AUDPC values in cases plants were inoculated with *Foln*3 alone or in combination of *Foln*3 + Fo47 strains or *Foln*3 + *Fol* 4287 strains. The capitals above the columns define statistically differences. Comparisons were done strain by strain (ANOVA, $P = 0.95$).
Fig. S4. *Fg*Ebr1 affects expression of genes in several gene clusters. Histograms represent mean relative expression levels from three replicate microarray experiments. Error bars represent standard deviation of the mean.
A. Expression means for genes from the *TRI* cluster in wild type PH-1 grown during wheat head infection (black bars) and in an *EBR1* deletion strain (white bars).
B. Expression means for genes from the aurofusarin biosynthetic cluster in wild-type PH-1 grown in complete medium (black bars) or for an *EBR1* deletion strain (white bars).
C. Expression means for genes from the butenolide biosynthetic cluster in wild-type PH-1 during wheat head infection (black bars) and in an *EBR1* deletion strain (white bars).
Table S1. Table containing all the numbered compounds in the Biolog wells. The boxed ones represent compounds on which the *Fo* Δ*ebr1* strain grows less than wild-type *Fol* 4287 The grey ones represent compounds on which the *Fo* Δ*ebr1* strain grows better than wild type *Fol* 4287.
Table S2. (A) *Fg* genes downregulated by more than fivefold in *Fg* Δ*ebr1* compared with *Fg* wild type PH-1 when grown in CM for 48 h. Values represent the average relative expression levels of each gene in wt and Δ*ebr1*. (B) *Fg* genes upregulated by more than fivefold in *Fg* Δ*ebr1* compared with *Fg* wild-type PH-1 when grown in CM for 48 h. Values represent the average relative expression levels of each gene in wt and Δ*ebr1*.
Table S3. (A) *Fo* genes downregulated by more than fivefold in *Fo* Δ*ebr1* compared with wild type *Fol* 4287 when grown in CM for 48 h. Values represent the average relative expression levels of each gene in wt and Δ*ebr1*. (B) *Fo* genes

up-regulated by more than fivefold in Fo Δ*ebr1* compared with wild-type *Fol* 4287. Values represent the average relative expression levels of each gene in wt and Δ*ebr1*.

Table S4. List of homologous *Fg* and *Fo* genes that show a similar or opposite expression pattern in *Fo* or *Fg* Δ*ebr1* compared with their respective wild types.

Table S5. FunCat analysis of genes that are > fivefold higher expressed in *Fg* wild-type PH-1 compared with *Fg* Δ*ebr1*. The categories in bold are significantly over-represented in the gene set ($P \leq 0.01$).

Table S6. FunCat analysis of genes that are > fivefold lower expressed in *Fg* wild-type PH-1 compared t *Fg* Δ*ebr1*. The categories in bold are significantly over-represented in the gene set ($P \leq 0.01$).

Table S7. FunCat analysis of genes that are > fivefold higher expressed in wild-type *Fol* 4287 compared with *Fo* Δ*ebr1*. The categories in bold are significantly over-represented in the gene set ($P \leq 0.01$).

Table S8. FunCat analysis of genes that are > fivefold lower expressed in wild-type *Fol* 4287 compared with *Fo* Δ*ebr1*. The categories in bold are significantly over-represented in the gene set ($P \leq 0.01$).

Table S9. (A) *Fg* genes downregulated by more than twofold in Δ*ebr1* compared with wt when grown *in planta* for 72 h. Values represent the average relative expression levels of each gene in wt and Δ*ebr1.* Gene names in bold are the genes from the TRI cluster found in this analysis. (B) *Fg* genes up-regulated by more than twofold in Δ*ebr1* compared with wt when grown *in planta* for 72 h. Values represent the average relative expression levels of each gene in WT and Δ*ebr1*.

Table S10. FunCat analysis of genes that are > twofold higher expressed in *Fg* wild-type *PH-1* compared with *Fg Δebr1* during *in planta* growth. The categories in bold are significantly over-represented in the gene set ($P \leq 0.01$).

Table S11. FunCat analysis of genes that are > twofold lower expressed in *Fg* wild-type PH-1 compared with *Fg* Δ*ebr1* during *in planta* growth. The categories in bold are significantly over-represented in the gene set ($P \leq 0.01$).

Table S12. (A) *Fol* 4287 homologues of *FTF1* and *FTF2*. Locus ID names are given as well as the chromosomes (Chr.) on which they are located. (B) *Fol* 4287 homologues of FGSG_06651. Locus ID names are given as well as the chromosomes (Chr.) on which they are located. (C) *Fol* 4287 homologues of FGSG_10517. Locus ID names are given as well as the chromosomes (Chr.) on which they are located.

Table S13. Primers used in this study.